JOURNAL OF MATERIALS SCIENCE 14 (1979) 2025–2052

Review
Thermophysical properties of oil shales

K. RAJESHWAR, R. NOTTENBURG, J. DUBOW
Department of Electrical Engineering, Colorado State University, Fort Collins, Colorado 80523, USA

Recent developments in the characterization of the thermophysical properties of various types of oil shales are reviewed. Changes in the thermal, mechanical and electrical properties of these technologically important materials are discussed, with temperature and organic content as the experimental variables. Structural models are presented to aid in predicting the variation of thermophysical parameters with organic content in the shale. Comparison of calculated results with experimental data are shown with thermal diffusivity as a representative parameter. Areas where further research of a fundamental nature would be of particular relevance are also highlighted in the review.

1. Introduction

The current search for alternative energy sources to petroleum has underlined the importance of oil shales as an economically viable substitute. Surveys by the United States Department of Interior indicate that there are over 700 billion barrels of economically recoverable synthetic crude oil spread over 17 000 square miles of Colorado, Utah, and Wyoming in the Green River Oil Shale Formation [1]. Non-commercial deposits occur beneath an additional 8000 square miles in these states. The total resources in this tri-state area constitute 1.8×10^{12} barrels of crude shale oil. Major oil-shale industries have also existed at various times in Manchuria, Australia, France, Scotland and Russia. It has been estimated that the reported occurrences of oil shale deposits number several hundred [2]. The tapping of hydrocarbon fuels from these vast resources would undoubtedly go a long way towards alleviating the current energy shortage in various parts of the world.

There are several accepted definitions for "oil shale." Oil shale has been defined [3] as a "compact laminated rock of sedimentary origin, yielding over 33% of ash and containing organic matter that yields oil when distilled, but not appreciably when extracted with ordinary solvents for petroleum." However, it has been pointed out that many oil shales so defined are not shales in the restrictive sense of fine-grained, fissile, clastic rocks; the mineral or textural features of many oil shales would allow them to be classified as other types of rock such as siltstone, impure limestone, black shale or impure coal [2].

The important oil shale deposits that have been characterized in various parts of the world are summarized in Table I. The lithology of oil shales, their depositional history, world distribution and resources have been described in recent reviews and monographs [2, 4–9].

From an energy point of view, the most important constituent of oil shales is the organic matter which is composed of both bitumen and kerogen*. The solubility of bitumen in common petroleum solvents makes its extraction a relatively easy matter although bitumen content in oil shale is only a minor fraction (usually $<5\%$). The bulk of the organic matter is composed of kerogen which is insoluble and inert. Retorting is therefore the most convenient method to extract hydrocarbon-like fuels from oil shales. Retorting technologies for processing oil shales have been dealt with in recent reviews [9, 10–14].

*The name "kerogen" was first applied by Brown in 1912 [16] to denote specifically the insoluble organic matter in oil shale. The specificity of this definition has however been lost in recent years (for example see [17]).

0022–2461/79/092025–28 $04.80/0

TABLE I Major oil shale deposits in the world*

Location of known deposits†	Geological era	Depositional conditions	Remarks
Northern Europe, northern Asia and east-central North America	Cambrian and Ordovician	marine-platform	Siliceous black shales yielding relatively small amounts of oil
Estonia, Leningrad	Ordovician		Thin, high-grade calcareous shales, rich in organic material
East-central United States	Silurian–Devonian	marine	Black shales yielding small amounts of oil ($40–80\ gal\ t^{-1}$)
Albert shales in eastern Canada	Carboniferous	lake-basin	Oldest reported tectonic lake-basin deposits
Southern Brazil (Irati shales) Uruguay, Southern Argentina	Late Permian	marine	One of world's largest oil-shale deposits
Northwestern United States (Phosphoria Formation)	Permian	marine	Low-grade in the black shale–phosphorite–chert assemblage
Central Africa (Stanleyville Basin of the Congo)	Triassic	fresh-water	High-grade lacustrine, interbedded with limestone and volcanic materials
Northeast Asia	Jurassic and Cretaceous	?	Associated with coal-bearing rocks
Israel, Jordan, Syria southern part of Arabian peninsula	Cretaceous	marine-platform	Black-shale–phosphorite–chert assemblage
Alaska, central Canada, western United States	Cretaceous	marine-platform	Largely low-grade
New Zealand, South American (Andean Mountains), western North America (Cordilleran and Coast ranges)	Tertiary	largely non-marine lake-basin	Associated with coal-bearing strata Generally low in grade
Colorado, Utah and Wyoming (Green River Formation)	Early and Middle	lake-basin	
Southern Brazil (Paraiba Valley), Yugoslavia (the Aleksinac deposits), Southern USSR, eastern China	Tertiary	lake-basin	
Algeria, Sicily, southern USSR (Caucasus region) southern California	Late Tertiary	marine	Diatomaceous shales with high bitumen content
New South Wales and Tasmania (Torbanite and Tasmanite deposits	Permian	fresh-water and marine	

*Data from [4], [6] and [7].
† Cannel shales and related deposits of Late Paleozoic Age are also known in Scotland, France, Spain, South America, Australia, USSR and in other countries.

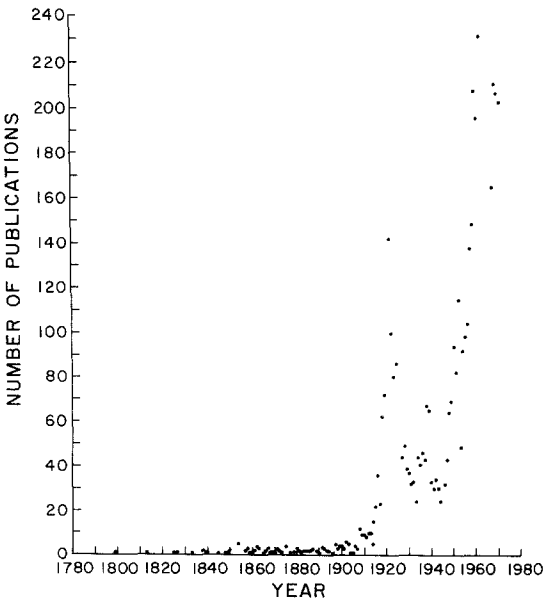

Figure 1 Number of publications and/or reports pertaining to oil shale (excluding patents) versus year of publication. (Data from *Chemical Abstracts* and *Engineering Abstracts*)

World-wide research in oil shale science and technology has undergone a rather unsteady advance since the first British patent which was issued in 1694 for extracting "oyle from a kind of stone" [15]. An examination of the trends in the number of publications and/or reports dealing with oil shale (excluding patents) that has appeared in the literature, shows essentially three periods of activity centered around 1920, 1950 and the late 1960s. This is shown in Fig. 1. The corresponding trends in oil shale research in the USA (as shown by the number of research reports and publications from the U.S. Bureau of Mines and Department of Energy) show remarkably parallel behaviour (Fig. 2). As seen in Figs. 1 and 2, interest in oil shales has been increasingly on the upsurge in recent years. A survey of the literature, however, reveals that a majority of investigations has dealt exclusively with shales of the Green River Formation. This is not altogether surprising in view of the tremendous resources of Green River oil shales.

Apart from the technological and geological aspects which have received a lot of attention, there is a need to develop a sound fundamental base for an understanding of the basic thermophysical properties of oil shales. Thermophysical measurements on oil shales are particularly important in view of the inherent nature of the methods that are commonly employed for extraction of the shale organic matter; these are mostly based on the application of heat for the pyrolysis of the organic matter in the shale. The effect of temperature on the properties of oil shales is thus crucial for efficient process design.

The term "thermophysical" is used in the present context to represent those parameters which are directly or indirectly related to the transport, the absorption or the release of heat. Properties such as thermal conductivity, thermal diffusivity and specific heat fall naturally into this definitive classification scheme. For materials which are thermally active, i.e., those which undergo thermal decomposition or phase transformation, (this is the case with oil shales in general), it is also necessary to characterize their thermal behaviour by thermo-analytical techniques such as differential thermal analysis (DTA) and thermogravimetry (TG). Electrical and mechanical properties have customarily become an integral part of thermophysical characterization in view of their extreme sensitivity to changes taking place in the material on application of heat. Thus, thermophysical properties in general can be broadly divided into three categories – thermal, electrical and mechanical, as shown in Fig. 3. These properties in turn encompass a wide spectrum of measurement parameters which can be correlated to yield a self-consistent picture on the overall thermophysical behaviour of the material of interest (Fig. 3). The relevance of thermophysical measurements to some typical on-field

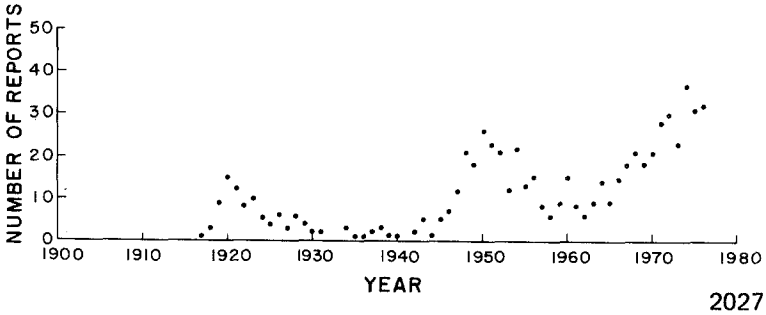

Figure 2 Number of research reports on oil shale from the US Bureau of Mines and the Department of Energy versus year of publication. [Data from USBM Report LERC/RI-77/7 (September 1977)].

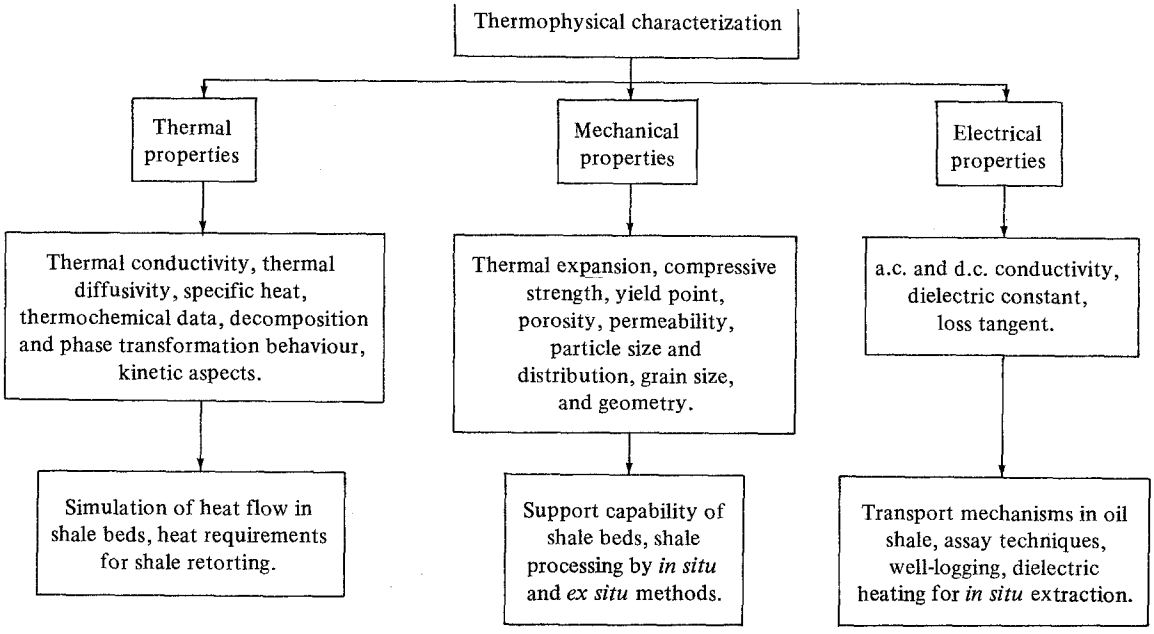

Figure 3 Classification of thermophysical properties and the relevance of measured parameters to on-field applications in oil shale technology.

applications in oil shale technology is also indicated in the same figure.

The present article reviews current knowledge on the thermal, electrical and mechanical properties of various types of oil shales. Variations in the thermophysical behaviour of these materials are discussed as a function of two variable parameters, namely temperature and organic content. Although the discussion focuses primarily on the oil shales of the Green River formation, comparisons with shales from other deposits are presented wherever sufficient data are available.

2. Thermal properties

2.1. Thermal decompcsition of oil shale kerogen

Thermal extraction of insoluble kerogen from the oil shale matrix is by far the most direct and simplest method for processing oil shales. The nature of the decomposition process, as with all thermally activated phenomena in general, can be conveniently studied from both mechanistic and kinetic points of view. These are discussed below.

2.1.1. Mechanistic aspects

Apart from the decomposition of the oil shale kerogen, there is a variety of other reactions that are brought about by application of heat. For example, the presence of a host of minerals in the oil shale matrix significantly complicates the thermal behaviour. The following reactions can be identified in general [5]: (a) evolution of water and gases; (b) conversion of kerogen to bitumen; (c) alteration of bitumen; (d) dissociation of bitumen to oils, gases and other compounds; (e) vaporization of oils; (f) burn-off of fixed carbon; (g) decomposition of organic residues and inorganic minerals.

The above reactions are critically dependent on the nature of the atmosphere surrounding the shale. For example, the oxidation of fixed carbon (Reaction f) can be effectively suppressed by excluding air or oxygen from the ambient (by flushing with an inert gas for example). The presence of even small amounts of air or oxygen will also lead to oxidative degradation of the shale organic matter commencing at temperatures as low as $\sim 200^\circ$ C [18]. The use of inert atmospheres, therefore precludes oxidation effects and facilitates a partial separation of the temperature regimes at which the above processes take place. The complexity of the kerogen decomposition process (Reactions b to e) is also compounded by the presence of secondary reactions which include secondary cracking and polymerization [19]. The rate of heating and the possible catalytic effects of mineral matter are additional complicating factors [20].

The exact mechanism by which kerogen transforms to bitumen (Reaction b) is a matter of some dispute. Thus it appeared from early studies that bitumen is formed in heavy solid or semi-solid form at a definite temperature depending on the type of shale [21]. However, later studies have shown that this transformation does not begin at any minimum temperature [22]. The amount of bitumen formed is also seen to bear a direct relationship to the time of heating of the material [23]. The temperature at which bitumen formation (from kerogen) has been reported is also variable. For example, McKee and Lyder [21] observe bitumen formation at 400–410° C for their shale samples. The results of Dulhunty [24] show a sharp increase in the rate of bitumen production at 360° C followed by a significant decrease at temperatures greater than 360° C. On the other hand, Hubbard and Robinson [25] present data which show that no kerogen is converted to soluble bitumen at temperatures below 325° C. Again in direct contradiction, two separate studies reveal that bitumen formation commences at temperatures as low as ~200° C [23, 26].

The discrepancies in the data reported by the above investigators could be traced to two possible factors influencing the transformation of kerogen to bitumen. The primary factor is the extreme sensitivity of the transformation mechanism to experimental conditions. It is possible that the results reported by various investigators pertain to widely differing experimental conditions and as such are not directly comparable. The influence of experimental variables such as atmosphere, etc. needs to be thoroughly investigated before any definite conclusions are drawn. This aspect because of its common impact on all thermophysical properties of oil shales will be discussed in greater detail in Section 5. A secondary factor contributing to conflict in the reported data is the possible variation in the chemical nature of the shale samples examined by different investigators. Alterations in the kerogen structure arising from differences in depositional history and age could influence its transformation temperature. However, for shales from the same location, as is the case for the Green River oil shales discussed above, such effects are likely to be minimal.

The nature of the bitumen initially formed by the thermal decomposition of oil shale kerogen is rather uncertain at the present moment. There is evidence for initial conversion of kerogen to an insoluble bitumen which transforms to soluble bitumen in a subsequent step [27, 28]. This intermediate step is not reported in most of the later studies on the thermal decomposition of oil shales. The inconsistency in the decomposition and properties of the primary product (or "pyrobitumen" as it is sometimes referred to) has led some workers to consider this material as a mixture of low temperature carbonization tar and undecomposed kerogen [28, 29]. There is also evidence which suggests that pyrobitumen has structural units linked by oxygen bridges; these bridges are ruptured at high temperatures producing a lower molecular weight soluble bitumen [30].

The temperature of conversion of bitumen to oils and gases, as with the formation of bitumen discussed above, is also critically dependent on experimental conditions. Oil shales which have the lowest C/H ratio have been shown to produce the largest amounts of oil from equal amounts of organic material [31]. The kerogens of marine sediments tend to yield more gas than the terrestrial shales on retorting because of a greater deficiency of hydrogen [32]. Retort products show a large variation when the nature of the shale is different; thus about two-thirds of the organic matter in Green River oil shales is converted to oils on pyrolysis while the oil yield of Swedish shales is less than 50% [5].

There are numerous reviews and reports in the literature on the characteristics of shale oils produced from different shales and retorting procedures [33–43]. A detailed discussion of the properties of shale oils is beyond the scope of this article.

2.1.2. Kinetic aspects

As with the mechanistic aspects discussed in the previous section, the results reported by various investigators on the kinetics of decomposition of oil shale kerogen reveal a spectrum of widely differing behaviour. This trend is reflected both in the postulated decomposition schemes (which range from simple one-step consecutive reactions to complicated branched schemes, Table II) and in the reported kinetic parameters (Table II). The wide variation in the values reported for the kinetic parameters is disturbing; the activation energies (E_a) calculated for the kerogen decomposition range from ~5 kcal mol^{-1} to 57 kcal mol^{-1}

TABLE II Various mechanisms postulated for the thermal decomposition of oil shale kerogen

Type of shale	Decomposition scheme	Reference
Green River	Kerogen $\xrightarrow{k_1}$ Bitumen $\xrightarrow{k_2}$ Oil, gas, and carbon	[25]
Green River	Kerogen $\xrightarrow{k_1}$ Gas, Bitumen, Carbon residue; $\xrightarrow{k_2}$ $(\text{Oil and gas})_{\text{liq.}}$; $\xrightarrow{k_3}$ $(\text{Oil and gas})_{\text{vap.}}$	[44]
Baltic	Kerogen $\xrightarrow{k_1}$ Pyrolytic bitumen $\xrightarrow{k_2}$ Residue; $\xrightarrow{k_2}$ Volatiles; $\xrightarrow{k_4}$ Volatiles	[45]
Green River	Kerogen $\xrightarrow{k_1}$ Rubberoid $\xrightarrow{k_2}$ Bitumen $\xrightarrow{k_3}$ Semicoke; $\xrightarrow{k_4}$ Gas; Rubberoid $\xrightarrow{k_4}$ Oil 1; Bitumen $\xrightarrow{k_6}$ Oil 2	[47]
Green River	Kerogen $\xrightarrow{k_1}$ Rubberoid $\xrightarrow{k_2}$ Bitumen $\xrightarrow{k_5}$ Semicoke $\xrightarrow{k_7}$ Coke; $\xrightarrow{k_4}$ Gas; $\xrightarrow{k_3}$ Oil; $\xrightarrow{k_6}$ Oil; $\xrightarrow{k_8}$ Heavy Oil $\xrightarrow{k_9}$ Oil; $\xrightarrow{k_{10}}$ Gas	[48]
Baltic	$\xrightarrow{k_{13}}$ Volatiles 6; $\xrightarrow{k_3}$ Asphaltenes 1 $\xrightarrow{k_{12}}$ Asphaltenes 3 $\xrightarrow{k_{15}}$ Malthenes 3 $\xrightarrow{k_{17}}$ Carboids 4; $\xrightarrow{k_{11}}$ Volatiles 5; $\xrightarrow{k_{14}}$ Carboids 3; $\xrightarrow{k_{16}}$ Volatiles 7; $\xrightarrow{k_6}$ Volatiles 3; Kerogen $\xrightarrow{k_2}$ Malthenes 1 $\xrightarrow{k_5}$ Asphaltenes 2 $\xrightarrow{k_8}$ Malthenes 2 $\xrightarrow{k_{10}}$ Carboids 2; $\xrightarrow{k_4}$ Volatiles 2; $\xrightarrow{k_7}$ Carboids 1; $\xrightarrow{k_9}$ Volatiles 5; $\xrightarrow{k_1}$ Volatiles 1	[46]

and the frequency factors span the range 10^2 to 10^{20} min^{-1}. Most of the investigations have described the kinetic behaviour in terms of a simple first-order equation. However, the inadequacy of the first-order law to take into account the experimental results in a satisfactory manner has been pointed out in recent studies [44, 46, 47, 51, 58]. The autocatalytic effect of the pyrolytic bitumen formed in the thermal decomposition of kerogen, is also apparent in the results obtained by some workers [44, 50, 58].

Most of the discrepancies in the reported data may be attributed to variations in the experimental procedure and improper recognition of the interfering factors resulting from such variations in the techniques. A critical appraisal of the reported results indicates that the following factors may be of importance in explaining the serious conflict in the literature data:

(a) The time required for the samples to attain the experimental decomposition temperature (in the case of isothermal experiments) introduces a significant error and must be taken into account (see for example [28] and [51]. While the "induction periods" are negligibly small at low temperatures where the duration of the decomposition is quite long, i.e., $t - t_0 \gg t_0$ (t_0 = induction period), they are a significant fraction of the total reaction time at higher temperatures. The use of small sample size (<50 mg) and efficient heat transfer aid considerably in alleviating this problem. Unfortunately, most of the investigations have employed rather large sample sizes for kinetic studies ([52] is a significant exception, but see below).

(b) The kinetic studies based on chemical analysis [22, 25, 49, 57] assume that the time required for the analysis does not significantly affect the observed results. Again, while this assumption may be valid at low temperatures,

considerable difficulties may be encountered at high temperatures where the pyrolysis is proceeding at an exceedingly fast rate.

(c) While several investigations have employed non-isothermal methods for the study of reaction kinetics (for example, [44, 52–55, 59]) the use of techniques involving a progressively changing temperature to determine a highly temperature dependent quantity (such as the rate of reaction) must be done with considerable caution and with full recognition of their inherent limitations [60, 61]. The poor fit of non-isothermal TG data to calculated results and the low E_a values observed in a recent investigation on Green River oil shale [54] have been attributed to the occurrence of "distinctly different processes occurring at the same time." However, the use of a simplified first-order expression to account for the observed results could also account for the discrepancies. The absence of any significant breaks in the peaks representing the rate of weight loss versus temperature also does not seem to support the occurrence of separate simultaneous reactions. Another investigation on the application of non-isothermal TG to the thermal decomposition of kerogen in Chattanooga shale, reports an increase in both E_a and frequency factor with increasing conversion [55]. These results have been interpreted in terms of (a) a catalytic effect of the initial decomposition products and (b) diffusional effects [55]. If autocatalytic effects were important, one would expect a rapid decrease and then an increase in E_a values with increasing conversion since the pyrobitumen concentration passes through a maximum and then decreases as the reaction progresses [44]. On the other hand, diffusional effects would result in a smooth decrease in E_a values with increasing conversion as the pyrolysis transforms the shale from a fairly impervious mass to a residue of highly porous friable ash. Since neither of these trends are apparent in the reported data, it is obvious that some other effect must play a part in accounting for the observed trends.

(d) The variation of activation energies and frequency factors with the extent of conversion of kerogen [52, 55] indicates that these parameters are only "apparent" values; such numbers, at best, are of only limited significance in a representation of the true kinetics of a chemical reaction. The use of the same sample at different temperatures (for isothermal experiments) employed in a recent investigation [52] is also open to question. This method necessarily assumes that the extent of the reaction has no effect on the subsequent kinetics; and/or that the products have no catalytic effect on the reaction kinetics. This assumption is definitely not borne out by the observed results or by the data reported in the literature [49, 50, 62]. At temperatures above 600° C, however, "reaction was much faster and a fresh shale sample was used for each temperature." The anomalous decrease in the rate constants for the high temperature pyrolysis observed in the above investigation [52] is also difficult to explain.

(e) The shift in the TG weight-loss curves with heating rate to lower temperatures with a decrease in the heating rate has been attributed to kinetic effects [55]. This effect is more likely due to variations in heat-transfer effects with changes in heating-rate [61]. An accurate representation of reaction kinetics from non-isothermal methods would be ideally independent of heating rate. Such conditions, however, are realized in practice only with the use of very small sample sizes and efficient control of heat transfer.

(f) The thermogravimetric method, employed in some studies [44, 62] utilizes a rather deep crucible to contain the oil shale samples. The large sample sizes employed in the investigation essentially means that the observed reaction rates are largely dependent upon both the ease of diffusion of the products and also upon the crucible. The authors' contention that the "rate of devolatilization would be independent of sample size if the material could instantaneously be raised to a given temperature" is also strictly not true. The behaviour, in the case of diffusion-limited reactions would be expected to be markedly dependent on sample size. In this regard the observed effects of sample size on weight-loss curves are significant [62].

(g) The marked effect of particle size on the rate of weight loss of oil shale samples reported in a recent study [53] merits further attention. The increase in the rate of weight loss and also in the extent of reaction with a decrease of particle size is significant. Similar effects have been noted by recent workers [44, 62] who show that doubling the particle diameter increases by a factor of about 4 the time required for 95% conversion of kerogen. Such trends in behaviour are strongly indicative of physical processes being of importance in controlling the reaction rate. Particle size

TABLE III Kinetic parameters for the decomposition of oil shale kerogen

Temp. range	Kinetic equation	Activation energy E_a (kcal mol^{-1})	Frequency factor (min^{-1})	Technique	Reference
350–525° C	$-\log_e(1-x) = kt + c$	13.572 (below 435° C)	$\sim 10^{20}$	Chemical analysis	[25]
		5.549 (above 437° C)	$\sim 10^{9}$		
150–350° C	$-\log_e(1-x) = kt + c$	19.0	–	Chemical analysis	[49]
350–525° C	Two first order and three second order equations	–	–	Mathematical analysis	[50]
430–475° C	$\log_e\left(\frac{1-x}{x}\right) = -kt + c$	40.5	–	TGA	[44]
400–525° C	$A \xrightarrow{k_1} B \xrightarrow{k_2} C$ (two consecutive first order equations)	$E_a^{(1)} = 10.65$	$\sim 10^{14}$	Analysis of literature data (inclusion of an induction period)	[51]
		$E_a^{(2)} = 42.45$	$\sim 10^{2}$		
316–440° C	Graphical integration	20–57.1	–	GLC and FID	[52]
350–425° C	First-order	48.5–54.0	$\sim 10^{12}$	Isothermal expts.	[54]
	Modified first-order	35.6–53.0	$\sim 10^{13}$	Non-isothermal methods	[54]
	$-\frac{1}{w_0}\frac{dw}{dt} = Ae^{(-E_a/RT)}f\left(\frac{w}{w_0}\right)$	57.1	–	Non-isothermal TGA	[54]
280–518° C	$-\log_e(1-x) = kt + c$	9.14	–	TGA	[53]
275–380° C	First order (autocatalytic)	52.80	–	Analysis of literature data	[29]
275–365° C	$-\log_e(1-x) = kt + c$	40.0	$\sim 10^{13}$	Chemical analysis	[22]
627–927° C	$-\log_e(1-x) = kt + c$	18.4	$\sim 10^{13}$	–	[56]
250–450° C	$-\log_e(1-x) = kt + c$	17.8	$\sim 10^{15}$	Chemical analysis	[57]

effects could also play an important role in the control of nucleation rate in heterogeneous solid decompositions [63]. The decrease in the extent of reaction with increasing particle size points towards the inhibiting effect of the reaction products on the further course of the decomposition. The transfer of heat to the larger particles also becomes extremely sluggish as a result of the low thermal conductivity of oil shale (see Section 2.2).

From a consideration of the factors outlined above, it is quite likely that the various activation energies listed in Table III refer to different rate-controlling processes each of which may be important under the conditions of the particular experiment. Thus the low activation energies (<10 kcal mol^{-1}) reported by some workers are possibly the result of physical processes (e.g. vaporization, gaseous diffusion) becoming the rate-limiting step for the overall decomposition reaction. Such processes are logically related to factors (f) and (g) above and can be facilitated by appropriate sample-holder design and by choice of optimal sample sizes. In this regard, it is interesting to note that although complex schemes have been proposed for the thermal decomposition of oil shale kerogen (Table II), none of the studies have clearly identified the manner in which each intermediate step may become rate-limiting under a particular set of experimental conditions. In the

ideal case, of course, the rate determining step should be related to a distinct bond-breaking process and as such must be unclouded by the effect of physical processes which are markedly dependent on experimental conditions.

The remarks in the preceding paragraphs highlight the need for a comprehensive study of the effect of variables such as sample size, specimen geometry, particle size, etc. on the decomposition kinetics of oil shale kerogen. This is particularly relevant to thermoanalytical techniques which have been employed in the past for kinetic studies on oil shale. The extreme variations in the kinetic parameters reported on the thermal decomposition of kerogen presumably arise from variations in the experimental techniques employed by different investigators; the results are also often clouded by the interfering effects of other variables. In view of this, it is doubtful whether the reported values reflect the true kinetic behaviour of oil shale kerogen. The representation of the kerogen decomposition in terms of a first-order model which has been adopted in most of the studies also does not provide an adequate explanation of the observed results. The applicability of a large number of kinetic laws governing the behaviour of gas–solid systems needs to be tested before a meaningful insight into the kinetics of kerogen decomposition can be gained.

2.1.3. Thermoanalytical studies

Thermoanalytical techniques such as DTA and TG are particularly useful for the characterization of the thermal behaviour of oil shales and oil shale minerals. It is usually desirable to modify commercially available instrumentation to tackle the specific problems associated with thermal analysis of oil shales and related fossil fuels. These problems can be classified under the following five headings [64]:

(a) Combustion, the burning of the shale organic matter during analysis.

(b) Re-condensation, the re-deposition and volatilization of evolving hydrocarbon gases.

(c) Property changes, the drastic alteration in physical and thermal characteristics of the shale during heating.

(d) Heterogeneity, the mixture of assorted minerals comprising oil shale.

(e) Representation, making an analysed sample represent a natural material.

Several examples for the development of special thermal analysis instrumentation for the study of oil shales and related materials exist in the current literature [64–76]. All these modified systems involve design features which permit elimination of one or more of the problems mentioned above. For example, use of thin flat pans as sample holders aids in a homogeneous temperature distribution, efficient control of the gaseous environment around the samples, and intimate contact with the temperature sensor when the oil shale samples are subjected to heat. Self-generated atmospheres and loss of good thermal contact arising from exfoliation of the shale samples are thus avoided by the use of flat pans [65].

In an inert atmosphere, the thermal decomposition of oil shale kerogen can be seen in the DTA trace as a weak endothermic effect around 500° C for most types of shales. The amplitude of the DTA peaks bears a direct relationship to the amount of organic matter in the shale [77, 78]. The loss of adsorbed moisture and occluded gases from the shale matrix is less easy to identify in a DTA or TG experiment. The heat effects and mass losses associated with these processes are quite small with the result that sensitivity requirements of the thermal analysis instrumentation become rather stringent. DTA curves of illitic shales have however shown the gradual loss of water associated with the indigenous clays present in these materials [76, 79].

The extreme sensitivity of the thermal behaviour of oil shales to atmospheric effects is demonstrated by the data obtained in this laboratory [18] on Green River oil shales. Fig. 4 shows the effect of the presence of air on the DTA curves of Green River oil shale. Fig. 4b shows the thermal behaviour of an oil shale sample heated in an inert atmosphere. The peak corresponding to kerogen decomposition is seen to be endothermic in nature. In the presence of air, however, (Fig. 4a) two exotherms are apparent, the first peaking at 439° C and the second at ~500° C. The first exothermic peak can be assigned to the combustion of light hydrocarbon fractions from the shale organic matter; the second exotherm arises from the burn-off of carbon coke.

2.1.4. Thermal characteristics of oil shale minerals

Thermal analysis methods have proved to be extremely useful for the identification and charac-

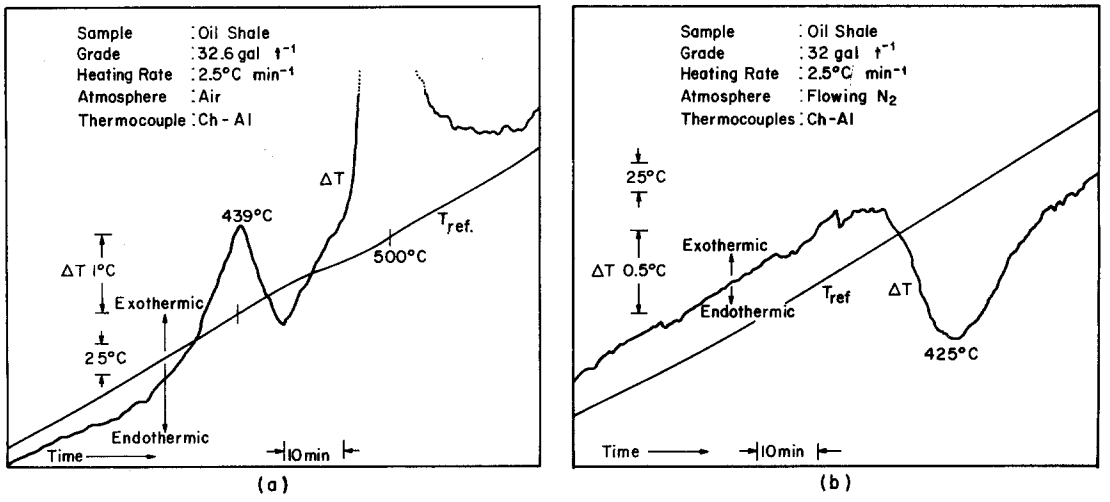

Figure 4 Effect of surrounding atmosphere on the thermal behaviour of Green River oil shale: (a) DTA in the presence of air and (b) DTA in an inert atmosphere of flowing N_2 [18].

terization of Green River oil shale and its constituent minerals [64–67, 70, 80–83].

Fig. 5 shows a superimposed DTA–TGA plot for a hypothetical oil shale sample containing a variety of minerals [65]. Most of the thermal effects shown in this figure arise from thermal degradation of the mineral constituents in the shale. The identification and quantification of complex carbonate minerals existing in the oil shales of the Green River formation such as "ferroan," ankerite and dawsonite by the use of thermal analysis techniques have been demonstrated recently [78, 84]. A gravimetric method has also been proposed for the quantitative determination of nahcolite and trona in Colorado oil shales [85]. This method is based on the loss of weight of the shale on heating at 105° C for 14 h. Although it has been claimed that other minerals do not interfere, recent experience in the authors' laboratory has shown that the initial moisture present in the shale is likely to cause errors which have to be corrected for [18].

Conflicting results are reported in the literature on the mechanism of the thermal decomposition of dawsonite. According to the results of some authors [86], dawsonite decomposes at 370° C according to the equation:

$$NaAl(OH)_2CO_3 \longrightarrow H_2O + CO_2 + NaAlO_2 \quad (1)$$

Another study on the thermal behaviour of dawsonite at temperatures between 290 and 330° C shows that the decomposition takes

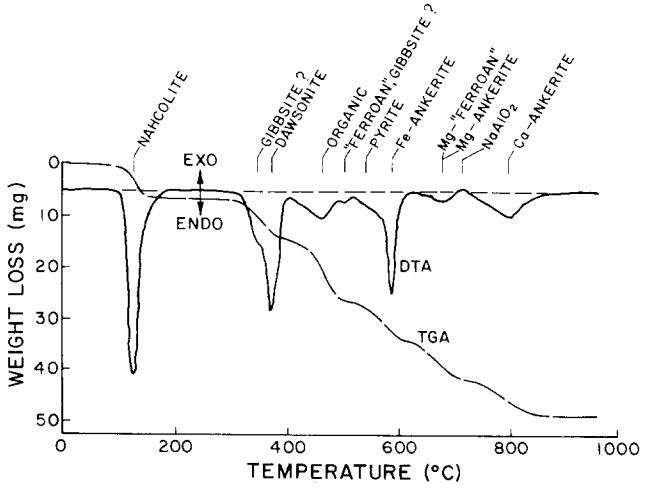

Figure 5 Simultaneous DTA–TG curves for oil shale showing the various thermal reactions of oil shale kerogen and of the constituent minerals [65].

TABLE IV Thermal characteristics of minerals commonly found in oil shale deposits

Minerals	Chemical formula	Type of thermal reaction	DTA peak* temperature (° C)	References
Calcite	$CaCO_3$	dissociation	860–1010	[90–103]
Dolomite	$CaMg(CO_3)_2$	dissociation	790, 940	[90, 95, 98 104–111]
Analcite	$NaAlSi_2O_6 \cdot H_2O$	dehydration, dissociation	150–400	[81, 90, 95 102, 112]
Shortite	$Na_2Ca_2(CO_3)_3$	dissociation	470	[83]
Trona	$2Na_2CO_3 \cdot NaHCO_3 \cdot 2H_2O$	dissociation, dehydration	170	[90]
Pyrite	FeS_2	oxidation, dissociation	550	[113]
Potassium feldspar	$KAlSi_3O_8$	dissociation	–	–
Gaylussite	$CaNa_2(CO_3)_2 5H_2O$	dehydration, crystallographic transformation, melting,	145, 175, 325, 445, 720–982	[114]
Illite	$KAl_4Si_7AlO_{20}(OH)_4$	dehydroxylation	100–150, 550, 900	[115, 116]
Plagioclase	$NaAlSi_3O_8 - CaAl_2Si_2O_8$	dissociation	–	–
Nahcolite	$NaHCO_3$	dissociation	170	[90, 102]
Dawsonite	$NaAl(OH)_2CO_3$	dehydroxylation, dissociation	300, 440	[65, 86–88]
Gibbsite	γ-$Al(OH)_3$	dehydroxylation	310, 550	[117–119]
Ankerite	$Ca(Mg, Mn, Fe)(CO_3)_2$	dissociation	700, 820, 900	[120]
Siderite	$FeCO_3$	oxidation, dissociation	500–600, 830	[61, 121, 122]
Albite	$NaAlSi_3O_8$	dissociation	–	–
Quartz	SiO_2	crystallographic transformation	~ 575	[123–125]

*In view of the dependence of DTA peak temperatures on experimental variables such as sample size, atmosphere, etc., the reported values represent only typical reaction temperatures.

place with the formation of Na_2CO_3 and Al_2O_3 [87]:

$$2NaAl(OH)_2CO_3 \longrightarrow Na_2CO_3 + Al_2O_3 + 2H_2O + CO_2 \quad (2)$$

The conflict in the literature results has been interpreted as arising from the two-step decomposition of dawsonite [88]. In the first step, it has been found that between 300 and 375° C, crystalline dawsonite decomposes with the evolution of all the hydroxyl groups and two-thirds of the carbon dioxide, leaving an amorphous residue. In the second rate-determining step, the balance of the CO_2 is released over the range 360 to 650° C producing crystalline $NaAlO_2$.

The reactions undergone by minerals and clays that are commonly found in oil shale deposits are summarized in Table IV. It must be noted that although the thermal characteristics of most of these materials have been well characterized in the pure state, interaction with shale organic matter and other minerals gives rise to significantly different thermal behaviour when associated the oil shale. Thus it has been found that dolomite and calcite minerals in oil shales decompose at temperatures which are ~250° C lower than those at which these minerals decompose in the "pure" state [89].

2.2. Thermal conductivity

Thermal conductivities of oil shales have been measured by techniques such as the transient line-probe method [126, 127], thermal comparator technique [128] and by dynamic heating methods [129, 130]. The range of temperatures and shale grades investigated in some instances is however quite limited [131–134]. Earlier studies, in addition, do not focus on the anisotropic nature

TABLE V Comparison of thermal conductivity values reported in the literature for Green River oil shales

Temperature range (° C)	Shale grade (litres t^{-1})	Orientation of shale bedding planes to heat flow	Range of thermal conductivity ($W m^{-1} ° C$)	Reference
25–75	166	not known	1.3–2.1	[133]
40	103	parallel	1.12 ~0.78	[134]
38–593	30–200	perpendicular parallel	0.69–1.56 (raw shales) 0.26–1.38 (retorted shales) 0.16–1.21 (burnt shales)	[126]
25–420	32–240	horizontal geometric mean	0.92–1.92 1.00–1.82 (raw shales) 0.17–1.63 (burnt shales)	[127]
38–205	43–189	parallel perpendicular	0.30–0.47 0.22–0.28	[129]
20–380	23–214	parallel perpendicular	1.00–1.42 (Anvil Points shales) 0.25–1.75 (Anvil Points shales) 0.50–1.50 (Logan Wash shales)	[128]

of heat conduction in oil shale (e.g. [131]). Recent studies have shown that the thermal conductivity, in directions which are parallel to the shale stratigraphic planes, is approximately ~30% higher than that in the perpendicular direction [128]. A summary of the literature data on the thermal conductivity of Green River oil shale is shown in Table V.

The results shown in Table V indicate that the thermal conductivities of retorted and burnt shales are lower than those of the raw shales from which they are obtained. The burnt shales are also found to have lower thermal conductivities than the corresponding retorted shales. These trends have been interpreted as being due to the fact that the mineral matter is a better conductor of heat than the organic matter and that the organic matter is a better conductor than the voids created by its removal [126]. While the first of the above hypotheses is reasonable when one takes into account the contribution of the lattice conductivity to the overall values, the effect of the amorphous carbon formed from the decomposition of the organic matter could also be of importance in explaining the difference in thermal conductivity values for retorted shales and the corresponding burnt samples. The role of voids in determing the magnitude of the thermal conductivity for oil shale is likely to be significant only for samples with high organic content.

The thermal conductivities of oil shales are, in general, only weakly dependent on temperature; the majority of studies report a gradual decrease with increasing temperature [126–128], although one study on Baltic shales reports an increase with increasing temperature [135]. Contribution to the overall thermal conductivity by radiative heat transfer could possibly explain this anomalous behaviour. Extreme caution is also to be exercised in the interpretation of results at temperatures close to the decomposition of the shale organic matter. For example, thermal conductivity values have been presented at temperatures around 400° C [127]. These values include the effects of decomposition of the shale organic matter although it has been claimed [127] that this is not a critical parameter as long as the rate of temperature increase of the sample is relatively slow. However,

TABLE VI Literature data on the thermal diffusivity of Green River oil shale

Technique	Range of thermal diffusivity values (10^2 cm^2 sec^{-1})	Temperature range (° C)	Range of shale grade (litres t^{-1})	References
Calculated from experimental thermal conductivity data	0.16–0.80 (⊥)* 0.26–0.83 (geometric mean)†	25–400	32–240	[127]
Transient-line probe	0.26–0.98 (raw shales) 0.13–0.88 (retorted shales) 0.10–0.72 (burnt shales)	38–260 38–482 38–593	28–202	[126]
Laser-flash	0.10–0.90	25–350	21–343	[137]

* Refers to heat flow in directions perpendicular to shale bedding planes
† Calculated from the equation $k_G^2 = k_\perp k_{11}$ where k is the thermal diffusivity and the subscripts G, ⊥, and 11 refer to geometric mean, perpendicular, and parallel, respectively.

the use of a steady-state parameter such as the thermal conductivity for describing the thermal behaviour of a sample undergoing decomposition is questionable and measurements in the temperature range where shale decomposition is known to occur, are likely to yield erroneous and irreproducible results.

The thermal conductivity values of oil shales show an inverse dependence on the amount of organic matter contained in them [126–128]. Equations have been proposed by various authors relating the thermal conductivity to the two variable parameters, namely temperature and shale grade. Thus Tihen *et al.* [126] recommend from statistical analyses the following equation for calculating thermal conductivities (K) of Green River oil shales assaying between 30 and 200 litres^{-1} within the temperature range 38–260° C for raw shales, 38–482° C for retorted shales and 38 to 593° C for burnt shales,

$$K = C_1 + C_2G + C_3T + C_4G^2 + C_5T^2 + C_6GT \quad (3)$$

where C_1 through C_6 are empirical constants, G is the shale grade in litres per ton and T is the temperature in °C. On the other hand, Prats and O'Brien [127] prefer a second-order polynomial in $(T-25)$ of the form

$$K = C_1 [1 - D_1(T-25) + D_2(T-25)^2] \exp(C_2G) \quad (4)$$

where C_1, C_2, D_1 and D_2 are again empirical constants. Simpler equations have been proposed for Baltic shales [136],

$$K = 1.30/G + 0.06 + 0.003\,T. \quad (5)$$

The above equations, apart from illustrating a general trend in the dependence of thermal conductivity on shale grade and temperature, have limited quantitative significance. Extrapolation of equations of this type to predict thermal conductivity of oil shales in general, is likely to result in serious error because of the observed dependence of the empirical constants on the nature of the shale, its origin, etc.

2.3. Thermal diffusivity

Literature data on the thermal diffusivity of Green River oil shales are fragmentary; available data are confined to three separate investigations (Table VI). Data on shales from other deposits also appear to be lacking in the current literature; although in favourable instances, the necessary values may be calculated from thermal conductivity and specific heat data through use of the equation

$$k = K/\rho c \quad (6)$$

where k is the thermal diffusivity, K is the thermal conductivity, c is the specific heat at constant pressure and ρ is the density of the material respectively.

The thermal diffusivity values show the same broad trends with variations in temperature and shale grade as do the thermal conductivities (Section 2.2), i.e., a decrease with increasing temperature and organic content in the shale. The retorted shales and burnt samples again show reduced thermal diffusivities relative to the raw materials (Table VI, [126]). The values reported by Prats and O'Brien (Table VI, [127]) have been calculated from Equation 6 from experimentally measured parameters although no corrections were made in their calculations for the variation of

TABLE VII Range of thermal diffusivities of oil shale minerals [138]

Mineral	Range of thermal diffusivity (10^2 cm^2 sec^{-1})	Temperature range (°C)	Anisotropic effects
Quartz	1.1–2.4	20–400	Not observed
Dolomite	0.3–1.5	20–500	Insignificant
Calcite	0.4–1.5	20–500	Insignificant
Plagioclase	0.4–1.2	25–510	Large in some cases
Low Albite	0.4–0.8	25–460	Small
Pyrite	4.6–8.0	25–360	Not observed
Analcite	0.4–0.5	25–360	Not observed
Potassium feldspar	0.4–0.7	32–280	Considerable

density with temperature. However, as these authors point out, this correction would tend to increase the calculated values somewhat. The calculational procedure (through use of Equation 6) often serves as a good check for the measured values as the data in [127] illustrate.

The laser flash technique has been found to be particularly suitable for measuring thermal diffusivities of oil shales [137]. Some inherent advantages of this method include elimination of thermal contact resistance problems and errors associated with the absolute accuracy of temperature sensors. The tendency of oil shale samples to exfoliate upon heating often results in loss of good thermal contact and this presents a serious problem with some techniques such as the transient line-probe method (see for example [126]).

The range of thermal diffusivities typically exhibited by oil shale minerals is shown in Table VII. These values were obtained by the laser-flash technique [138]. The high diffusivity values characteristic of pyrite are to be noted. Oil shale samples containing significant amounts of pyrite are thus likely to show rather high thermal diffusivities.

2.4. Thermochemical data

2.4.1. Specific heat

Early work on the specific heat of American oil shales is restricted to limited ranges of temperatures and shale grades [21, 133]. Later studies [136, 139] report specific heat dependence on temperature and shale grade, typified by equations of the type

$$C_p = 0.172 + (0.067 + 0.00162\,G)\,10^{-3}\,T \quad (7)$$

$$C_p = 0.178 + 0.00138G + 0.0004T \quad (8)$$

for raw shales and

$$C_p = 0.174 + 0.051 \times 10^{-3}\,T \quad (9)$$

for "spent" or retorted shales. Equations 7 and 9 refer to Green River shales whereas Equation 8 pertains to Baltic shales.

The numerical constants in the above equations, as with those in equations previously listed in Section 2.2, represent values for shales for specific locations in the particular formation.

Considerable increases in the specific heat values with increasing organic content have been observed in the above-mentioned studies although the relative contributions of the various oil shale constituents to the overall values are somewhat uncertain. Specific heat values for Green River kerogen are not available in the literature although such values have been calculated from atomic heats for Glen Davis (Australia) kerogen [140].

2.4.2. Heat content and heat of retorting

Heat requirements for processing oil shales may be determined from the heat contents [142] and heats of decomposition of their constituent minerals and organic matter [143]. The heats of retorting so obtained are overall values and include the contributions from [143]:

(a) heat content of the mineral matrix and other non-volatile portions of the shale at the retort temperature,

(b) heat of reaction for the conversion of shale organic matter into gas, oil and coke,

(c) heats of decomposition of the minerals in the shale which decompose under the experimental conditions,

(d) heats of vaporization of oil and water, and

(e) heat content of the gas and oil vapours at the temperature of their exit from the retort chamber.

The last contribution presents a significant source of error which has to be corrected for in the experimentally determined heat of retorting values. Apparently this has not been done in some of the studies (for example [144]). The available

TABLE VIII Values reported for heat of retorting of Green River oil shales

Heat of retorting ($cal\,g^{-1}$)	Shale grade ($litres\,t^{-1}$)	Reference
398–430	?	145
57–210	98, 195	144
139–167	33–137	142

data on Green River oil shales are compiled in Table VIII. The reported heat of retorting values show the expected increase with increasing shale grade and temperature; the disparity in the range of values observed by different investigators possibly reflects differences in the composition of the shale samples. It should be borne in mind that the presence of minerals which decompose at temperatures below the range at which the organic matter is thermally extracted, would increase the heat requirements for processing shales containing these minerals. Thus it has been estimated that nahcolite and dawsonite containing shales would require an additional $177\,cal\,g^{-1}$ and $215\,cal\,g^{-1}$ respectively [142]. Heat requirements for retorting oil shales containing 15% analcite would be increased by about 6% [81].

Thermochemical data on oil shales from other deposits appear to be limited to the torbanite shales of the Glen Davis formation [140, 146] and to the kukersite shales from Estonia [147].

3. Mechanical properties

Oil shales in general are quite impermeable and non-porous. The highly consolidated nature of these materials and the significant absence of micropore structure, pore volume and internal surface are revealed in nitrogen absorption and desorption studies [148]. The distribution of the organic matter within the inorganic matrix is essentially inter- and not intra-particle. Estimates made from surface area data also seem to suggest that only a small amount of the organic matter is bonded either physically or chemically to the mineral constituents. On the other hand, results obtained from compressive strength measurements indicate a high degree of inorganic cementation between the mineral particles comprising each lamina and between adjacent lamina [149].

Mechanical properties of oil shales such as porosity, permeability, and compressive strengths are markedly dependent on temperature and organic content [149, 150]. Studies on oil shale rubble under retorting conditions indicate that samples assaying less than $69\,l\,t^{-1}$ experience only minor reduction in permeability whereas richer shales (100 to $200\,l\,t^{-1}$) lose essentially all permeability [151, 152]. Similar studies on porosity changes on heating have shown a substantial increase in the porosity values which is directly proportional to the temperature of heating and the shale grade [153, 154]. Samples heated to elevated temperatures (to drive off the organic matter and carbonate minerals) show greater increases in porosity values relative to the raw shales [155]. Attempts at improving the permeability of raw shales by acid leaching of the mineral carbonates have not been entirely successful [153, 154], although similar methods bring about two-fold increases in the porosity [153].

Most oil shales in a stress-free environment undergo expansive deformation under application of heat. This deformation, which is a function of both organic content and temperature, has been found to be extensive in rich oil shales, whereas in lean oil shales (assaying less than $48\,l\,t^{-1}$), the deformation is minor [151]. The lean shales in addition exhibit mechanical recovery effects over a wide temperature range and in some cases, the samples also seen to show simultaneously and to varying degrees, elastic and viscoelastic properties along with plastic deformation [151]. In general, thermal expansion and exfoliation effects characteristically observed for oil shales are accompanied by the generation of fissures which are caused by failures due to thermal stresses and by the release of combustible gases from the samples [156]. These effects are particularly pronounced at temperatures where the organic matter starts to decompose (usually in the range 400 to 485° C).

Changes in the compressive strengths of oil shales on heating are characterized by pronounced anisotropic effects. Compressive strengths are, in general, greater in directions parallel to the shale stratigraphic planes which indicate that the stress propagation paths in these materials are critically dependent on their orientation relative to the shale bedding planes [157].

Interesting effects are observed in the mechanical properties at temperatures immediately prior to the kerogen decomposition. Pronounced changes in the electrical properties at these temperatures seem to indicate the presence of a structural transformation in which the kerogen molecules essentially commence to dissociate

themselves from the inorganic matrix [157]. This transition which is usually observed at ~380° C for Green River oil shales seems to be primarily physical rather than chemical in origin; an observation which is supported by the relatively small loss of organic matter at these temperatures [151].

4. Electrical properties

Changes in the electrical parameters of oil shales as a function of temperature and other chosen variables, often yield valuable information on the mechanistic aspects of the physical and chemical processes taking place in these materials on application of heat. The extreme sensitivity of electrical methods of analysis is an added advantage in this regard. Both a.c. and d.c. methods can be employed although a.c. techniques are preferable in view of their capability to detect and resolve various polarization mechanisms in the material.

Measurements on various types of oil shales in d.c. electric fields have shown an exponential decrease in resistivity values as a function of temperature [157–159]. These trends are typically characteristic of ionic solids which conduct by a thermally activated transport mechanism. The presence of a variety of minerals in the oil shale matrix makes it rather difficult to identify conclusively the current carrying ions in the material, although the close correspondence of activation energies at high temperatures (>380° C) with those typically observed for carbonate minerals seems to indicate that carbonate ions could be a major current transporting species [157]. However, estimates made from such data are at best speculative and must be considered with due caution. Apart from a strict thermally activated enhancement in the oil shale conductivity, the chemical changes in the material as a result of heat could also influence its conduction behaviour. Thus changes in the resistivity (from 10^{10} Ω cm at room temperature to 10 Ω cm at 900° C) of Russian shales have been attributed to the breakdown of hydrocarbon units in oil shale kerogen [158, 159]. The dramatic effect of chemical reactions in oil shales on their electrical conduction behaviour is illustrated by the results shown in Figs. 6 and 7. Fig. 6 shows results for raw Green River oil shales and Fig. 7 depicts data for the reheated materials. The broad minima in the resistivity curves at temperatures in the range 40 to ~380° C (Fig. 6) arise from the gradual loss of free moisture and water molecules bonded to

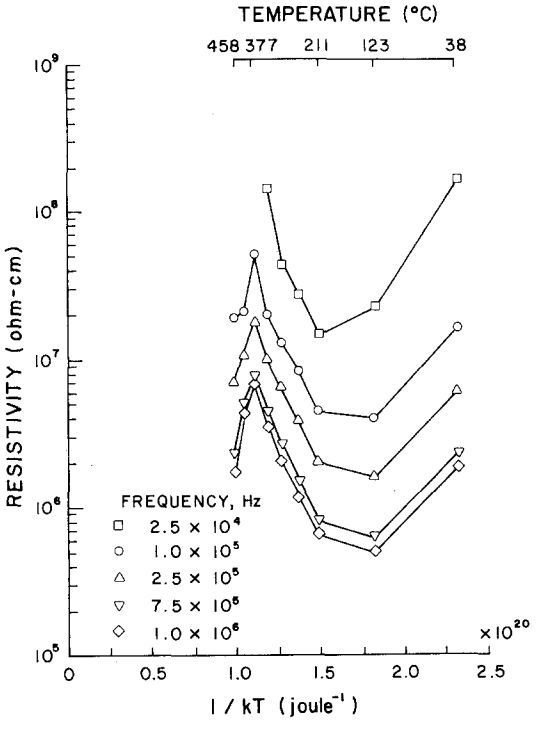

Figure 6 Frequency-dependent behaviour of electrical resistivity (ρ) as a function of reciprocal temperature for a 117 litres t^{-1} shale sample [157].

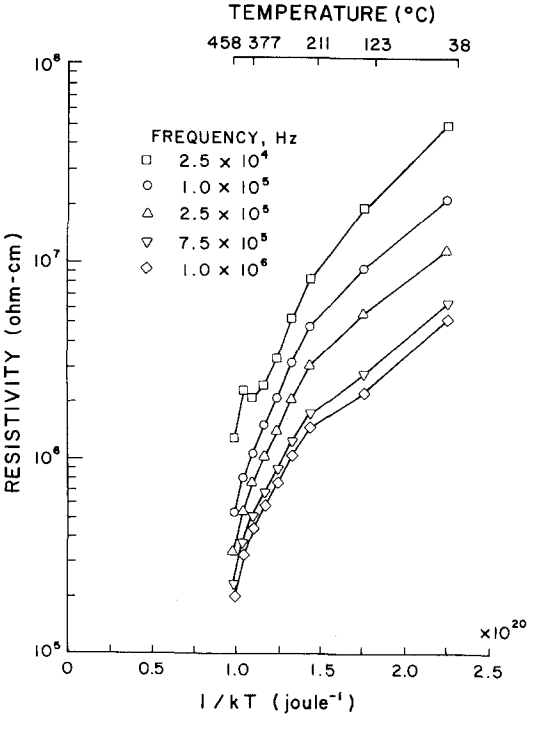

Figure 7 Same plot as in Fig. 6 for the sample reheated in a second cycle [157].

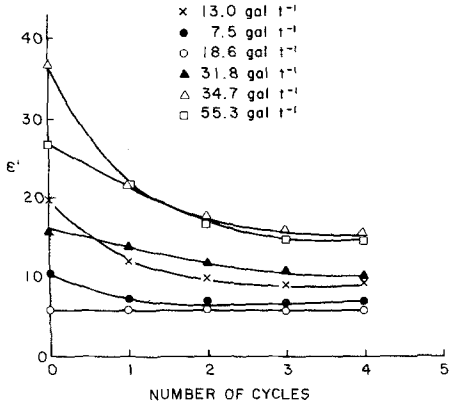

Figure 8 Variation of dielectric constant (ϵ') with number of heating cycles for several grades of Green River oil shales [164].

the clay particles in the shale matrix. The peaks in the resistivity immediately following these minima correspond to the structural transformation discussed in Section 3. The subsequent decrease in the resistivity values arises from the breakdown of the kerogen macromolecular structure as a result of thermal decomposition (cf. above results on Russian shales). The same shale samples on cooling back to room temperature and reheating back to ~500° C exhibit the usual Arrhenius behaviour typical of ionic solids (Fig. 7). Note that the resistivity minima and the peaks have disappeared; the smooth decrease in the resistivity values now arises solely from the thermally activated conduction discussed above.

The dielectric constants (ϵ') of oil shales show interesting behaviour as a function of temperature and frequency. Anomalously high dielectric constants are observed for these materials at low temperatures; these high values have been attributed by some workers to electrode polarization effects [160]. A more likely explanation is the occurrence of interfacial polarization (e.g. Maxwell–Wagner type) in these materials arising from the presence of moisture and as a result of accumulation of charges at the sedimentary varves in the shale. These effects are clearly seen in recent results [70, 161] on Green River oil shales (Figs. 8 and 9). Fig. 8 shows the dielectric constants of several oil shale samples of varying organic content as a function of the number of heating cycles. (Each cycle consists of heating the samples at 110° C for 24 h and cooling back to room temperature prior to testing). A marked decrease in ϵ' values with each subsequent drying cycle is evident. Fig. 9 shows the dispersion behaviour of ϵ' as a function of prior thermal treatment. The degree of frequency dispersion at each heating cycle attests to the appreciable effect of moisture on interfacial polarization mechanisms in oil shale.

Figs. 10 and 11 show typical trends in the variation of ϵ' with temperature for Green River oil shales [161]. The ϵ' values initially show a smooth decrease with temperatures up to ~250° C (Fig. 10) whereafter they increase again (Fig. 11) attaining values comparable to those observed initially for the raw shales. The initial decrease in ϵ' values is probably caused by the gradual release of adsorbed moisture and chemically

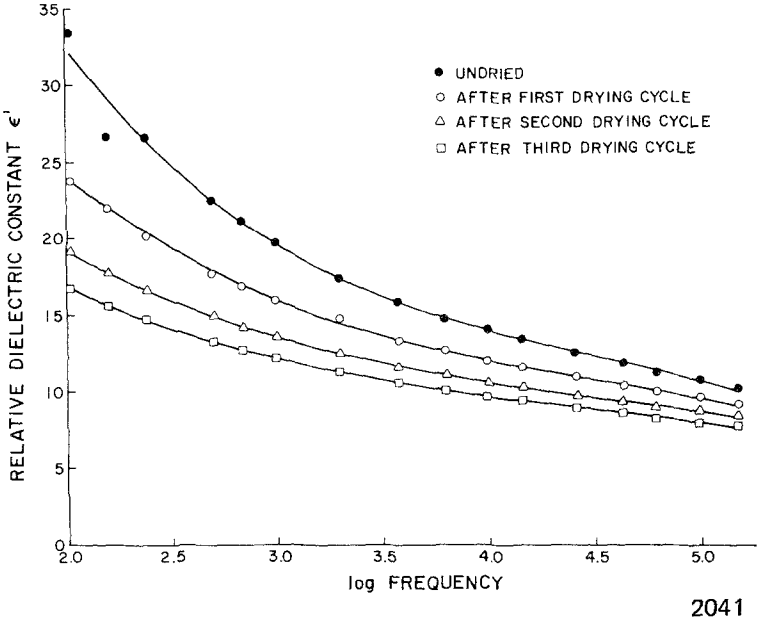

Figure 9 Variation of ϵ' with frequency and thermal treatment for Green River oil shales [164].

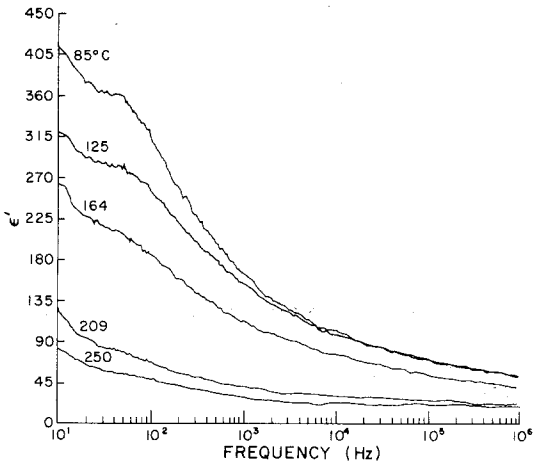

Figure 10 Frequency and temperature dependence of ϵ' at low temperatures (< 250° C) [161].

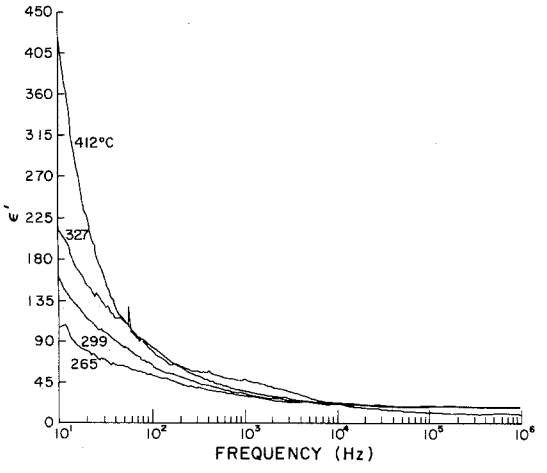

Figure 11 Frequency and temperatures dependence of ϵ' at high temperatures (> 250° C) [161].

bonded water from the oil shale matrix (cf. results on resistivity changes, Fig. 6). The subsequent increase in ϵ' with increasing temperature (Fig. 11) could be attributed to three factors:

(a) Increased orientational freedom of the kerogen molecules arising from their dissociation from the mineral particles in the oil shale matrix.

(b) Build-up of carbon in the material as a result of thermal decomposition of the organic matter in the shale, and

(c) Presence of a space-charge layer in the material at elevated temperatures arising from blocking of current carriers at the electrodes.

It is possible that all three mechanisms could operate synergistically. Evidence of electrode polarization effects at high temperatures is provided by the characteristic occurrence of a low frequency "spike" or cut-off in the plots of dielectric loss factor, ϵ'' versus temperature and frequency (Fig. 12). Such spikes are typical of blocking electrode effects [162].

Interfacial polarization effects in oil shales as mentioned above, can arise from the presence of either moisture or sedimentary varves in the materials. The occurrence of broad peaks in the loss tangent at low frequencies (<1000 Hz) provides additional support for this hypothesis. Typical trends in the variation of loss tangent (tan δ) with frequency and temperature are shown in Fig. 13. The peaks in tan δ at elevated tempera-

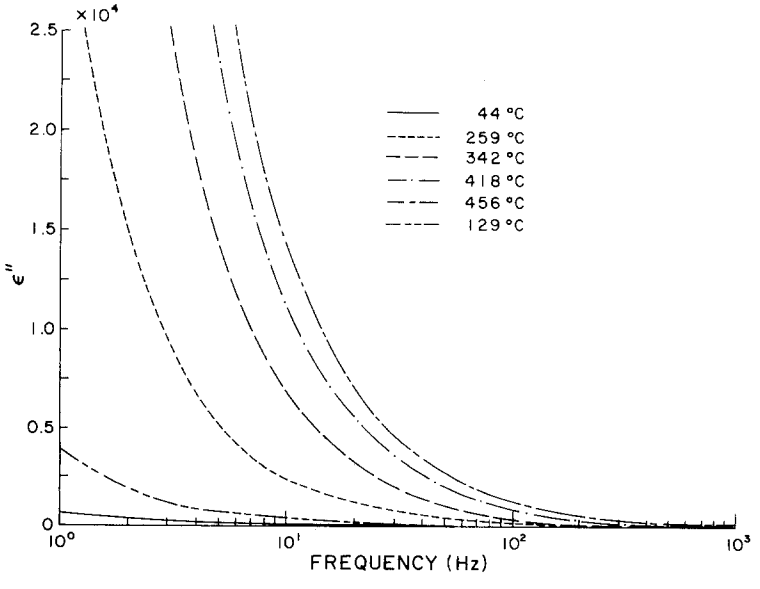

Figure 12 Representative plot showing the variation of the loss factor, ϵ'' with frequency at different temperatures [161].

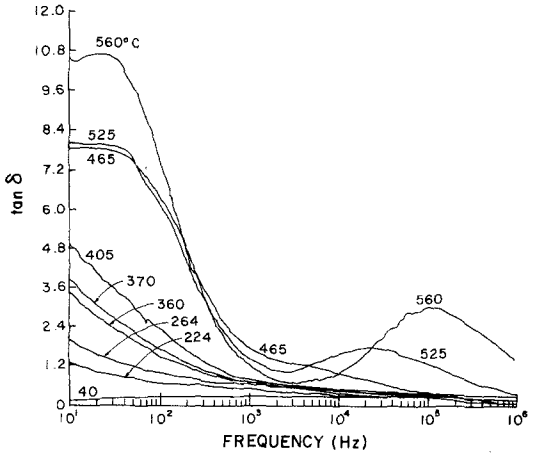

Figure 13 Dispersion in loss tangent, tan δ for a 89 litres t^{-1} oil shale sample at different temperatures [71].

tures appear to be related to dipolar relaxation effects arising from the increased orientational freedom of kerogen molecules [71].

Literature data on the dependence of dielectric parameters (e.g. ϵ', ϵ'', tan δ) on shale grade are in sharp conflict. Conclusions based upon investigations on a limited number of shale grades [163] have been recently shown to be in serious error [164]. Claims as to a smooth dependence of ϵ' and ϵ'' on shale grade [163, 165] are not supported by recent measurements on a wide range of shale grades at frequencies extending from 50 Hz to the microwave region [166]. It is possible that earlier measurements were clouded by effects of moisture or similar artifacts. As a clear illustration of the extent to which such effects could be misleading, results for ϵ' as a function of shale grade and drying cycle are presented for two measurement frequencies, 100 Hz and 1 MHz respectively in Figs. 14 and 15. These data show that it is clearly invalid to postulate a dependence of ϵ' on shale grade based on measurements with undried samples spanning a limited range of shale grades.

The failure to trace a clear-cut dependence of dielectric parameters on shale grade could be attributed to interfering effects from geometrical variables (e.g. pore structure, varve geometry, etc.) and the presence of moisture. In this regard, the extreme sensitivity of electrical properties to such effects proves to be a serious handicap. Thermal and mechanical properties, on the other hand are much less sensitive to statistical variations in geometrical and structural features of the test material.

5. General discussion

A summary of the trends in the variation of the thermophysical properties of oil shales as a function of temperature and organic content is shown in Table IX. It must be noted that almost all the studies reported in the literature are in essential agreement as to the general trends illustrated in Table IX. The major disparity in the results reported by various investigators lies in the magnitude of the measured parameters representing the various thermophysical properties of oil shales. This is reflected in the reported kinetic parameters (Table III), thermal conductivity values (Table V), thermal diffusivities (Table VI), and in thermochemical data (Table VIII). The factors contributing to inconsistencies in the reported data are possibly many-fold and it is unlikely that any one factor taken in isolation could completely account for the conflict in the results. To cite an example, the extreme variations in the kinetic parameters

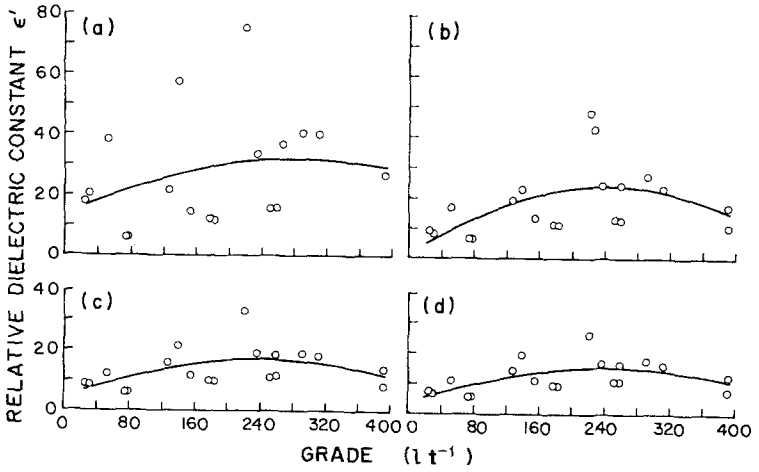

Figure 14 Dependence of ϵ' (at 100 Hz) on the amount of organic matter in the shale: (a) undried samples, (b) after one heating cycle, (c) after two heating cycles, and (d) samples subjected to three heating cycles [164].

TABLE IX Summary of the trends in the variation with temperature and organic content for thermophysical parameters of oil shales*

Thermophysical parameter	Temperature	Organic content
Thermal conductivity	↓	↓
Thermal diffusivity	↓	↓
Specific heat	↑	↑
Heat of retorting	↑	↑
Porosity	↑	↑
Permeability	↓	↑
Compressive strength	↓	↓
Electrical conductivity	↑↓↑†	?
Dielectric constant	↓↑†	?
Loss tangent (or loss factor)	↑	?

*↑ and ↓ indicate respectively an increase and decrease in the measured values with *increasing* temperature and shale grade.

†The sequence of indicated changes partly reflects chemical changes taking place in the shales.

reported for the thermal decomposition of oil shale kerogen probably arise from gross variations in the experimental techniques employed by different investigators. These results, on the other hand, are also simultaneously clouded by effect of other variables of a "material" origin such as particle size, chemical composition and so on. In view of this, it is important to realize that the values reported for the various thermophysical parameters of oil shales are to a large extent

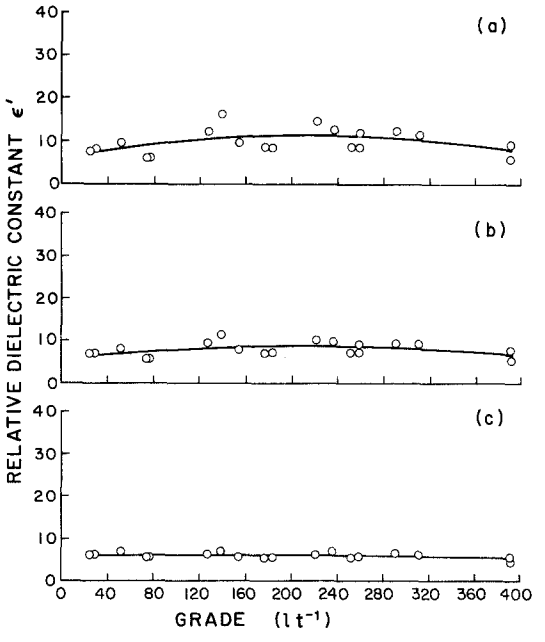

Figure 15 Dependence of ϵ' (at 1 MHz) on the amount of organic matter in the shale: (a) undried samples, (b) samples subjected to two heating cycles, and (c) after four heating cycles [164].

"apparent" or "procedural." While this may be true for all materials in general, the difficulty in obtaining "real" values for oil shales and similar naturally-occurring materials is compounded by the wide spectrum of variations in their chemical composition and by their heterogeneous nature. Similar arguments may be put forward to resolve the conflicting mechanisms proposed for the thermal decomposition of oil shale kerogen (Section 2.1.1). It is possible that each proposed mechanism may be valid under a particular set of experimental conditions and for a specific shale type. However, the consensus of opinion points toward the complex nature of kerogen decomposition in general and the occurrence of complicating side reactions, the relative importance of which is dictated by the conditions employed in the particular experiment.

In spite of the above-mentioned difficulties in the correlation of data obtained from various sources, it is sometimes useful to model the behaviour of oil shales from a fundamental viewpoint – such an approach has the inherent advantage of providing a working hypothesis from which to compare and contrast all experimental data. Thus, although extensive experimental data on the thermal, electrical and mechanical properties are available for oil shales in general and for Green River shales in particular (Sections 2 to 4), several questions relating to the variation of parameters representing these properties have not been answered up to this point. Can oil shale be effectively modelled as a heterogeneous two-phase material with the organic matter representing one phase and the composite minerals representing the second phase and if so, how are the various minerals combined to form the second phase? What is the geometric distribution of the two phases in the oil shale matrix? From a knowledge of the thermophysical parameters of the two separate phases, can we predict the corresponding values for the whole? What are the factors influencing the observed anisotropic behaviour in the thermal, electrical and mechanical properties of oil shales?

We will attempt to answer these equations with the help of working models which have been drawn from the literature and which are suitably modified to apply for the specific case of oil shales. For comparison with experimental data, we will choose thermal diffusivity values as a function of shale grade, although the conclusions

reached therein may be equally well applied to explain the variation of the other thermophysical parameters discussed in Sections 2 to 4.

Following the approach of Tsao [167] and Cheng and Vachon [168], we consider a unit cube of oil shale and slice it into thin layers as shown in Fig. 16a. The dispersed material (which we assume in the present case to be the mineral phase) is then collected into strips as shown in Fig. 16b. The additivity of conductivities in parallel means that the slices would have the same conductivity in either Fig. 16a or b. Also, any rearrangement of the order of slices in the cube would have no effect on the overall thermal resistance in view of the additivity of resistances in series. For a parabolic distribution of the disperse mineral phase in the continuous organic matrix, one can make use of the equation derived originally by Cheng and Vachon [168]:

$$1/k_e = 2\int_0^x \frac{dx}{k_0 + (k_m - k_0)y} + \frac{1-2x}{k_0} \qquad (10)$$

where

k_0 = thermal diffusivity of the organic (continuous) phase

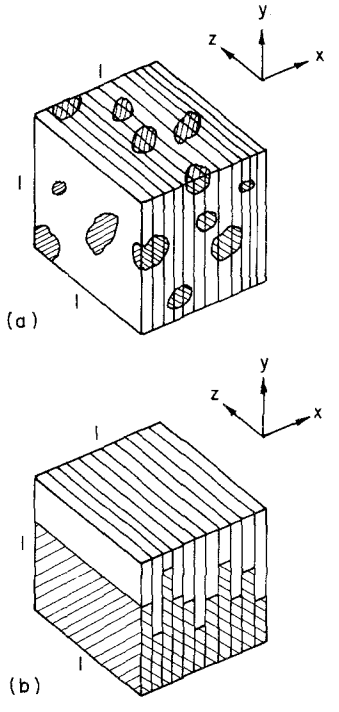

Figure 16 (a) A unit cube of the oil shale sample sliced in thin layers. (b) The disperse mineral phase then rearranged as shown [167, 169].

k_m = thermal diffusivity of the mineral (disperse) phase

k_e = thermal diffusivity of the oil shale sample

In Equation 10,

$$y = B + Cx^2 \qquad (11)$$

where the set of constants B and C can be evaluated from the appropriate boundary conditions for the particular volume fraction of the disperse phase, ϕ_m. The constant B is, in all cases found to be unity and C is always negative [169]. Defining a new constant such that $C = -C'$, we have from Equation 11

$$y = 1 - C'x^2 \qquad (12)$$

Substitution of Equation 12 in Equation 10, evaluating the integral and rearranging (see [169] for details of calculations) yields

$$\frac{1}{k_e} = \frac{2}{[k_m C'(k_m - k_0)]^{1/2}} \times \log \left\{ \frac{\left[\frac{k_m}{C'(k_m - k_0)}\right]^{1/2} + x}{\left[\frac{k_m}{C'(k_m - k_0)}\right]^{1/2} + x} \right\} + \frac{1-2x}{k_0} . \qquad (13)$$

Equation 13 enables us to calculate the thermal diffusivity of an oil shale sample from a knowledge of the thermal diffusivities of its constituent phases and their appropriate volume fractions.

The next problem is to estimate an overall effective value for the thermal diffusivity of the mineral particles in the disperse phase. The minerals commonly found in oil shale deposits of the Green River formation and a typical mineral distribution in oil shale samples are shown in Table X. The thermal diffusivities measured for these minerals by the laser flash method (Table VII)

TABLE X Typical distribution of minerals in Green River oil shales and their thermal diffusivity values at 25° C

Mineral	wt %	Thermal diffusivity* (10^2 cm^2 sec^{-1})
Dolomite	32	1.31
Illite	19	1,90
Calcite	16	1.39
Quartz	15	2.29
Albite	10	0.75
K-feldspar	6	1.53
Pyrite	1	7.86
Analcite	1	0.44

*Data from [138]. See also Table VII.

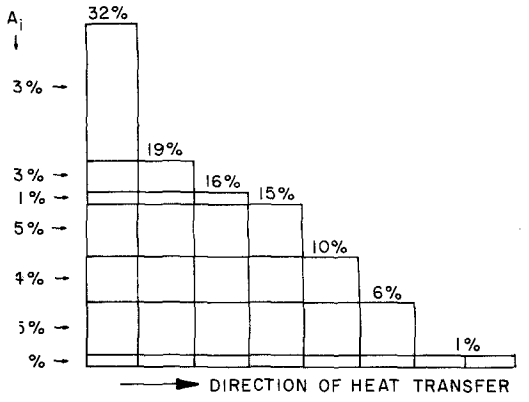

Figure 17 Combination of the various minerals in the oil shale matrix showing the fraction of each mineral in a parallel configurations (A_i) relative to the direction of heat flow [169].

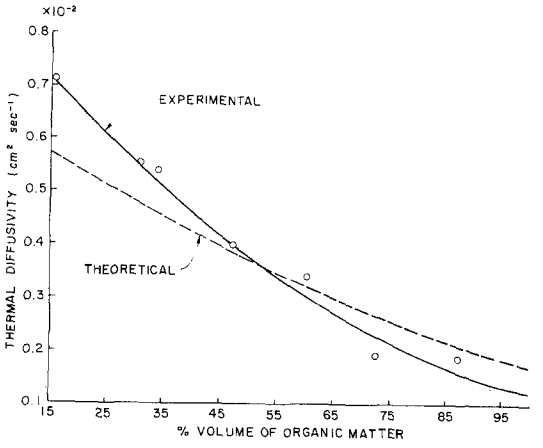

Figure 18 Comparison of the theoretical curve (Equation 13) with experimental data for the thermal diffusivity of Green River oil shales (heat flow is in directions perpendicular to the shale varve structure) [169].

are also shown in the same table. We next combine the experimental values assuming the additivity of resistivity in series and conductivity (or diffusivity) in parallel according to the equation:

$$\frac{1}{k_m^{eff}} = \sum_i \frac{A_i \phi_m^i}{k_m^i} \qquad (14)$$

where

k_m = thermal diffusivity of each mineral listed in Table X
ϕ_m = volume fraction of each mineral
A_i = fraction of each mineral which happens to be parallel (c.f. Fig. 17)
k_m^{eff} = effective thermal diffusivity of the mineral disperse phase.

The summation in Equation 14 is carried out over all the minerals shown in Table X.

For the typical mineral distribution shown in Table X, the value of k_m^{eff} turns out to be 0.240×10^{-2} cm^2 sec^{-1}. It must be pointed out that the value of k_m^{eff} obtained from Equation 14 is lower than that obtained from a "pure" combination of resistivity in series (see below).

The value for the thermal diffusivity of the organic (continuous) phase, k_0, is taken from an extrapolation of the experimental thermal diffusivity versus organic content data towards the high organic content (>350 l t^{-1}) region. This turns out to be 0.181×10^{-2} cm^2 sec^{-1}. Substitution of numerical values for k_0 and k_m^{eff} in Equation 13 then enables one to compute the overall effective thermal diffusivity k_{eff}, for each volume fraction of the organic (or mineral) phase. This is shown in Fig. 18 where the computed thermal diffusivity values are compared with the experimental thermal diffusivity data (taken from previous work carried out in this laboratory, [137]) as a function of the percentage volume fraction of the organic phase.

The thermal diffusivities and thermal conductivities of Green River oil shales exhibit anisotropic behaviour; the values for heat flow in directions parallel to the shale sedimentary varves are seen to be about 20 to 30% higher than that for directions perpendicular to the sedimentary varve structure (Section 2.2). Considering a segment of an oil shale sample, we can divide it into a set of resistances arranged in parallel or series depending on the direction of heat flow as shown in Fig. 19. In a physical sense then, we have the situation where each sedimentary varve in the oil shale sample, represents regions of high thermal resistance to heat flow. Neglecting contact resistances between the individual varves, we then have the lower and upper bounds respectively for the overall thermal diffusivity (or conductivity) according to the equations:

$$\frac{1}{k_e^{\perp}} = \frac{\phi_0}{k_0} + \sum_i \frac{\phi_m^i}{k_m^i} \qquad (15)$$

$$k_e^{\parallel} = \phi_0 k_0 + \sum_i \phi_m^i k_m^i \qquad (16)$$

where $k_e^{\parallel}$ is the overall thermal diffusivity for heat flow in directions perpendicular to the shale varve structure (cf. Fig. 19a) and $k_e^{\parallel}$ is the thermal diffusivity of the oil shale sample for heat flow in

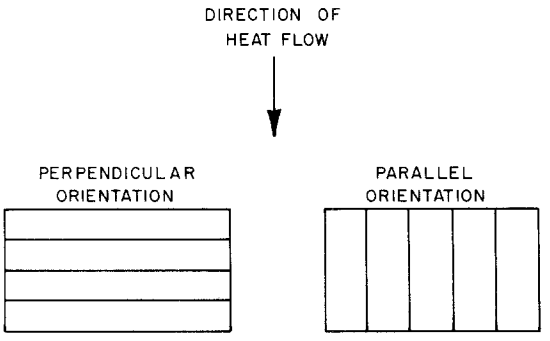

Figure 19 Representation of the oil shale varve structure in terms of (a) resistances arranged in series and (b) resistances arranged in parallel. "Perpendicular" and "Parallel" refer to the direction of heat flow with respect to the orientation of sedimentary varves in the shale sample [169].

directions parallel to the sedimentary varve structure (cf. Fig. 19b). The summation in Equations 15 and 16 is again carried over all the minerals present in the shale.

Substituting numerical values for k_0 (0.181×10^{-2} cm^2 sec^{-1}) and the weighted thermal diffusivities of the various minerals (cf. Table X), we can compute $k_e^{\perp}$ and $k_e^{\parallel}$ as a function of the volume of organic matter in the shale. This is shown in Fig. 20 where the theoretical curves are compared with experimental data. While the experimental data for heat flow in perpendicular directions are in good agreement with the theoretical curve, the marked discrepancy between theory and experiment for the parallel situation is evident. Two factors (somewhat interrelated) could contribute to this: (a) the resistances are not arranged in a strict parallel configuration as shown in Fig. 19b; i.e. there could be a mixed series–parallel arrangement which would tend to lower $k_e^{\parallel}$ from that predicted by Equation 16; (b) similar considerations would apply to the total thermal diffusivity of the mineral matrix, k_m^{total} (i.e. the second term in the right-hand side of Equation 16). A lower effective value for the mineral matrix (cf. Equation 14) would decrease $k_e^{\parallel}$ towards the experimental data points. Thus the computation of k_m^{total} assuming an idea parallel configuration for the mineral matrix would result in a value which overestimates that existing in the real case.

An alternative approach to the above problem would be to take recourse to "intermediate formulae" which would result in k_e values intermediate between the two bounds given by Equations 15 and 16 (cf. Fig. 20). We choose for this purpose firstly the geometric mean model which is given by the equation:

$$k_e = k_m^{\phi_m} k^{\phi_0} \qquad (17)$$

Again substituting numerical values for k_m and k_0 in the above equation, k_e is computed as a function of ϕ_0. The resultant curve is shown in Fig. 21. A substantial improvement in the agreement with experimental data is evident except at low levels of organic content ($< \sim 135\,l\,t^{-1}$).

Another formula derived originally by Maxwell [170] gives the conductivity of a random distribution of solid spheres in a continuous medium. This formula, again assuming the minerals to form the discontinuous phase as before, is given by:

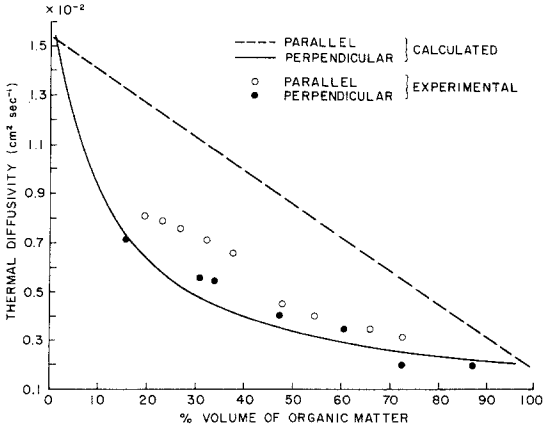

Figure 20 Comparison of the theoretical curves (computed from Equations 15 and 16) with experimental data for heat flow in directions parallel and perpendicular to the shale varve structure [169].

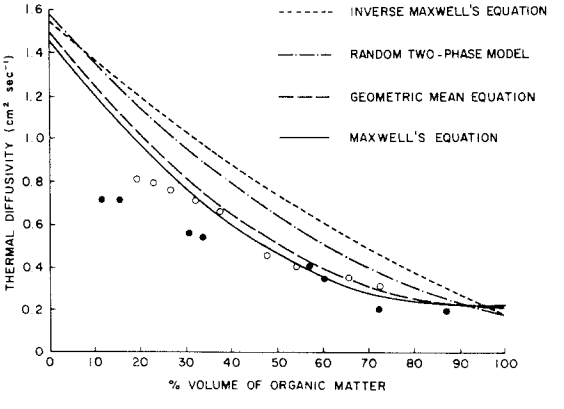

Figure 21 Comparison of the trends in the variation of thermal diffusivity with organic content predicted by Maxwell's equation, inverse Maxwell's equation and the geometric mean model with experimental data [169].

$$k_e = \frac{k_0\left[1-2\phi_m\left(\frac{1-k_m/k_0}{2+k_m/k_0}\right)\right]}{\left[1+\phi_m\left(\frac{1-k_m/k_0}{2+k_m/k_0}\right)\right]} \quad (18)$$

A plot of k_e versus ϕ_0 using the above equation is shown in Fig. 21. Agreement with experimental data is again good except for low volume fractions of organic phase.

We now assume the organic matter to represent the disperse phase in oil shale and treat the composite mineral phase as the continuous medium. In this case, we have the so-called "inverse Maxwell's equation" which is given by the following:

$$k_e = \frac{k_m\left[3k_0/k_m + 2\phi_m(1-k_0/k_m)\right]}{\left[3-\phi_m(1-k_0/k_m)\right]} \quad (15)$$

The behaviour of k_e as a function of ϕ_0 (i.e. $1-\phi_m$) as predicted by the above equation is shown in Fig. 21. The marked discrepancy between this model and the experimental data and the good agreement shown by Equation 18 justify our original assumption that the organic matter forms the continuous phase and the minerals form the disperse phase in oil shales.

We will now treat oil shale as a completely random two-phase assembly having regions of both the mineral and organic phases in the correct proportions which are embedded in a random mixture of the same two phases, i.e. no assumptions are made as to the spatial continuity of one phase. The equation appropriate to this case has been derived by Brailsford and Major [171]; which after correcting for a numerical error in their paper, reads:

$$k_e = \tfrac{1}{4}\{(3\phi_m-1)k_m + (3\phi_0-1)k_0 + [\{(3\phi_m-1)k_m + (3\phi_0-1)k_0\}^2 + 8k_mk_0]^{1/2}\} \quad (20)$$

This relation is also shown in Fig. 21 after substitution of the appropriate numerical values in the above equation. The lack of good agreement with experimental data shows that the geometric distribution of the two phases in oil shales is not completely random. This important result yields additional justification for the assumption of ordering and spatial continuity of one phase in oil shale. (This assumption is implicit in the use of Equations 13 and 15–19).

We will now compare the relative merits of the various models discussed above in predicting the variation of the thermal transport parameters of oil shales with the amount of organic matter contained in them.

From the results shown in Fig. 18, we see that the Cheng and Vachon model shows departures from the experimental data at low and high levels of organic content in the shale. For shales of medium grade containing between ~40 and 65 vol% of organic matter (corresponding to Fischer assay values of 120 and 250 l t^{-1}, respectively), agreement between theory and experiment is seen to be satisfactory. Most of the shale deposits of commercial interest in the Green River formation are of medium grade so that the Cheng and Vachon model (Equation 13) can be used to predict the variation of thermal transport properties with organic content for these oil shales without incurring serious error.

It is of interest to examine the validity of the assumptions made originally by Cheng and Vachon in their derivation of Equation 13 in the present context of oil shales. Oil shales, especially at room temperatures exhibit negligible porosity [153] so that assumption (4) (in [168]) is valid. The absence of porosity and the relatively low temperatures we are considering in the present case also effectively mean that thermal convection and radiation effects can be neglected so that assumption (2) in Cheng and Vachon's paper is justified. In the absence of evidence to the contrary, it is also reasonable to assume that the discontinuous phase in uniformly dispersed in the continuous phase in the case of oil shales (assumption (5) in [168]). On the other hand, assumptions (3) and (7) in Cheng and Vachon's paper, (namely that contact resistance between the two phases is negligible and no chemical interaction takes place between the disperse and continuous phases respectively) are likely to introduce difficulties in the case of oil shales*. Prior work [148] has yielded evidence for the occurrence of chemical interaction between the organic and mineral phases in oil shales so that assumption (7) is clearly unjustified. The errors introduced by the failure of assumptions (3) and (7) could account for the departure from

*Contact resistance between the disperse and continuous phases is not specific to oil shales alone and must be taken into account for all composite materials, synthetic or otherwise.

experimental data at high and low levels of organic content (cf. Fig. 18).

We have to consider contact resistance effects not only between the organic and mineral phases but also between the various minerals themselves especially at high levels of mineral content (or low levels of organic content). The departure shown by the geometric mean model (Equation 17) from the experimental data, for shales with less than 40 vol% organic matter (cf. Fig. 21) is possibly a direct manifestation of this effect. At higher levels of organic content, this equation gives a good estimate of the variation of thermal transport parameters, for heat flow in directions both parallel and perpendicular to the shale stratigraphic planes.

Maxwell's equation (Equation 18) with the minerals as the disperse phase and the organic matter as the continuous phase, yields equally satisfactory results for oil shales containing organic matter higher than ~35 vol% (cf. Fig. 21). The failure of this equation at lower organic levels (which correspond to packed-bed values of the disperse mineral phase) can be again traced to the initial assumptions made in the derivation of this equation [170]. Maxwell's expression is not applicable for large volume fractions of the disperse phase where the interactions between the particles constituting the disperse phase can no longer be ignored.

It must again be emphasized that we can use any convenient thermophysical parameter e.g. thermal conductivity, dielectric constant, compressive strength, etc. to carry out the calculations detailed above. The choice of thermal diffusivity in the preceding examples merely reflects the availability of sufficient data for the various constituents of oil shales. The use of electrical parameters for modelling studies is currently limited by the lack of reliable experimental data on the dependence of electrical properties on shale grade (Section 4).

Although the above calculations have been carried out only for the variation of thermophysical parameters with shale grade, the effect of the other variable parameter, i.e. temperature, may conceivably be taken into account in the modelling studies. Information derived from structural investigations of oil shale kerogen [33, 172, 173] would be of particular relevance to such studies. However, the extremely complex nature of the kerogen macromolecular network complicates matters considerably. Elucidation of the exact mechanism by which the various segments of the network are broken by temperature poses an interesting fundamental problem. This is an area of research where a concerted effort by researchers from widely differing disciplines (e.g. solid state physics and chemistry, organic chemistry, geochemistry, polymer science, physical chemistry) should hopefully provide the necessary answers over the next few years.

6. Concluding remarks

Extensive thermophysical data are available at present only for oil shales of the Green River formation. Difficulties in the correlation of data reported by various investigators on oil shales in general, may be attributed to variations in experimental techniques, the extreme sensitivity of the thermophysical behaviour of these materials to ambient conditions and to inconsistencies in material properties such as chemical composition, previous history, etc. In this regard, it is useful to adopt a unified approach to the study of these materials with the aid of empirical or semi-empirical models such as the ones discussed in the previous section. Further research on a more fundamental level will undoubtedly contribute to a better understanding of the nature of these complex materials and also will enable their efficient utilization.

Acknowledgements

This project was carried out with financial support from NSF (RANN) and the Department of Energy. The authors are grateful to Y. Wang, M. Freeman and R. Rosenvold for providing valuable experimental and technical support and to Jim Weber, John Duvall, Remo Tisot, Don Johnson and others at the Laramie Energy Research Center for many stimulating discussions.

References

1. T. F. YEN and G. V. CHILINGARIAN in "Oil Shale," edited by T. F. Yen and G. V. Chilingarian (Elsevier Publishing Co., Amsterdam, 1976) Ch. 1.
2. D. C. DUNCAN, *ibid.* Ch. 2.
3. J. M. GAVIN, "Oil Shale" (Washington Government Printing Office, 1924).
4. F. C. JAFFE, *Colorado School of Mines, Miner. Ind. Bull.* 5 (1962).
5. D. R. WILLIAMSON, *ibid.* 7 (1964).

6. D. C. DUNCAN and V. E. SWANSON, *U. S. Geol. Surv. Circ.* **523** (1965).
7. G. OZEROV, "Progress and Prospects in the Utilization of Oil Shale," U. N. Dept. Econ. Soc. Aff., Resour. Transp. Div., New York, Paper 1 (1965).
8. T. F. YEN (ed.), "Science and Technology of Oil Shale" (Ann Arbor Science Publishers, Michigan, 1976).
9. T. A. SLADEK, *Colorado School of Mines, Miner. Ind. Bull.* 17 (1974).
10. C. H. PRIEN in "Oil Shale," edited by T. F. Yen and G. V. Chilingarian (Elsevier Publishing Co., Amsterdam, 1976), Ch. 12.
11. C. H. PRIEN, *Ind. Eng. Chem., Annual September Issue*, **40** (1948) **55** (1963).
12. D. R. WILLIAMSON, *Colorado School of Mines, Miner. Ind. Bull.* 8 (1965).
13. G. U. DINNEEN and G. L. COOK, *Tech. Rev.* 76 (1974) 26.
14. G. U. DINNEEN in "Oil Shale," edited by T. F. Yen and G. V. Chilingarian (Elsevier Publishing Co., Amsterdam, 1976) Ch. 9.
15. M. EELE, British Patent No. 330 (1964).
16. A. CRUM-BROWN in "Geological Survey Memoirs" (Scotland) (H. M. Stationery Office, London, 1927) p. 160.
17. R. F. CANE, *Nature* **228** (1970) 1009.
18. K. RAJESHWAR, Unpublished results (1977).
19. J. D. SAXBY in "Oil Shale," edited by T. F. Yen and G. V. Chilingarian (Elsevier Publishing Co., Amsterdam, 1976) Ch. 6.
20. A. J. CARLSON, University of California (Berkeley) Publications in Engineering **3** (1921) 613.
21. R. H. McKEE and E. E. LYDER, *Ind. Eng. Chem.* **13** (1921) 613.
22. C. G. MAIER and S. R. ZIMMERLEY, *Utah Univ. Res. Inv. Bull.* **14** (1924) 62.
23. A. J. FRANKS and B. D. GOODIER, *Quart. Colorado School of Mines,* 17 Suppl. A (1922).
24. J. A. DULHUNTY, *Proc. Roy. Soc. (NSW)* 76 (1943) 268.
25. A. B. HUBBARD and W. E. ROBINSON, *USBM Rept. Inv.* **4744** (1950).
26. T. C. HOERRING and P. H. ABELSON in "Organic Geochemistry," Carnegie Inst. Ann. Rep., Geophys. Lab. Yearbook **62** (1963) p. 229.
27. R. H. McKEE and P. L. V. MANNING, *Oil Bull.* **13** (1927).
28. A. YA. AARNA, *Trudy Tallin Politekh. Inst.* **57** (1954).
29. A. K. MITYUREV, "Chemistry and Technology of Combustible Shales and Their Products" (Translated from Russian by I. Geller), Office of Technical Services, Washington, D.C., Document OTS 61–11434 (1962).
30. A. YA. AARNA and K. A. KASK, *Zhur. Priklad. Khim* **29** (1956) 764.
31. T. E. DANCY and V. GIEDROYC, *J. Inst. Pet.* **36** (1950) 593.
32. J. M. HUNT and G. W. JAMIESON, *Bull. Am. Assoc. Pet. Geol.* **40** (1956) 1477.
33. W. E. ROBINSON and K. E. STANFIELD, *USBM Inform. Circ.* (1960) 7968.
34. R. H. McKEE, "Shale Oil" (Chemical Catalog Co., New York, 1925).
35. G. U. DINNEEN, J. R. SMITH and G. W. BAILEY, *Ind. Eng. Chem.* **44** (1952) 2647.
36. W. E. CADY and H. S. SEELIG, *Ind. Eng. Chem.* **44** (1952) 2636.
37. P. L. COTTINGHAM, *Ind. Eng. Chem.* **15** (1976) 197.
38. J. C. STAUFFER, Ph.D. Thesis, Columbia University, New York (1926).
39. T. F. YEN, *Adv. Chem. Series* **151** (1976).
40. J. J. CUMMINS, F. G. DOOLITTLE and W. E. ROBINSON, *USBM Rept. Inv.* **7924** (1974).
41. *Idem, ACS Preprints, Div. Fuel Chem.* **20** (1975) 154.
42. S. L. CHONG, J. J. CUMMINS and W. E. ROBINSON, *ibid.* **21** (1976) 265.
43. J. J. CUMMINS and W. E. ROBINSON, *ibid.* **21** (1976) 94.
44. V. D. ALLRED, *Chem. Eng. Prog. Symp. Ser.* **62** (1966) 55.
45. A. Ya. AARNA, *Zhur. Priklad. Khim.* **28** (1955) 1138.
46. A. I. SHUL'MAN and V. A. PROSKURYAKOV, *Khim. Teknol. Goryuch. Slantsev. Prod. IKh. Pereab.* (1968) 278.
47. W. F. JOHNSON, D. K. WALTON, H. H. KELLER and E. J. COUCH, *Quart. Colorado School of Mines* **70** (1975) 237.
48. W. D. SCHNACKENBERG and C. H. PRIEN, *ind. Eng. Chem.* **45** (1953) 313.
49. J. J. CUMMINS and W. E. ROBINSON, *USBM Rept. Inv.* **7620** (1972).
50. D. W. FAUSETT, J. H. GEORGE and H. C. CARPENTER, *ibid.* **7889** (1974).
51. R. L. BRAUN and A. J. ROTHMAN, *Fuel* **54** (1975) 129.
52. A. W. WEITKAMP and L. C. GUTBERLET, *Ind. Eng. Chem.* **9** (1970) 386.
53. R. A. HADDADIN and F. A. MIZYET, *ibid.* **13** (1974) 332.
54. J. H. CAMPBELL, G. KOSKINAS and N. STOUT, Lawrence Livermore Lab. Rep., UCRL-52089 (1976).
55. A. Y. HERRELL and C. ARNOLD Jr, *Thermochim acta.* **17** (1976) 165.
56. British Patent Spec. 677140 (to Standard Oil Development Co.) August 13 (1952).
57. L. DERICCO and P. L. BARRICK, *Ind. Eng. Chem.* **48** (1956) 1316.
58. D. FINUCANE, J. H. GEORGE and H. G. HARRIS, *Fuel* **56** (1977) 65.
59. C. ARNOLD Jr., Sandia Lab. Energy Rep., Sand 75–0154 (1975).
60. J. H. SHARP, in "Differential Thermal Analysis," Vol. 2, edited by R. C. MacKenzie (Academic Press, New York, 1972) p. 47.
61. P. D. GARN, "Thermoanalytical Methods of Investigation" (Academic Press, New York, 1965).

62. V. D. ALLRED and G. I. NIELSON, *Chem. Eng. Prog. Symp. Ser.* **61** (1965) 60.
63. P. W. M. JACOBS and F. C. TOMPKINS in "Chemistry of the Solid State," edited by W. E. Garner (Butterworths, London, 1956) Ch. 7.
64. J. W. SMITH and D. R. JOHNSON in "Thermal Analysis," edited by R. F. Schwenker, Jr and P. D. Garn (Academic Press, New York, 1969), p. 1251.
65. *Idem,* in "Proceedings of Second Toronto Symp. on Thermal Analysis" edited by H. G. McAdie (Chemical Institute of Canada, Toronto, 1967), p.95.
66. *Idem, U.S. Govt. Res. Quart. Rep.* **71** (1971) 61.
67. *Idem, Amer. Lab.* **3** (1971) 8.
68. M. MÜLLER-VONMOOS and R. BACH in "Thermal Analysis," edited by R. F. Schwenker, Jr and P. D. Garn (Academic Press, New York, 1969) p. 1229.
69. P. C. UDEN, D. E. HENDERSON and R. J. LLOYD in "Proceedings of the 1st European Symp. on Thermal Analysis," edited by D. Dollimore (Heyden & Sons, London 1976) p. 29.
70. K. RAJESHWAR, R. NOTTENBURG and J. DUBOW, *Thermochim. Acta.* **26** (1978) 1.
71. R. NOTTENBURG, M. FREEMAN, K. RAJESHWAR and J. DUBOW, *J. Solid State Chem.* **27** (1979) in press.
72. *Idem, Anal. Chem.* (1979) in press.
73. W. L. WHITEHEAD and I. A. BREGER, *Science* **111** (1950) 279.
74. P. L. WATERS, *Nature* **178** (1956) 324.
75. R. L. STONE and H. F. RASE, *Anal. Chem.* **24** (1957) 1273.
76. R. L. STONE, *Anal. Chem.* **32** (1960) 1582.
77. H. HEADY, *Amer. Mineral.* **37** (1952) 804.
78. D. R. JOHNSON, N. B. YOUNG, and J. W. SMITH, LERC/R1–77/6.
79. W. W. BLACK, *Trans. Leeds. Geol. Assoc.* **7** (1958) 111.
80. J. W. SMITH and D. R. JOHNSON, *USBM Rept. Inv.* **7429** (1970).
81. D. R. JOHNSON, N. B. YOUNG and W. A. ROBB, *Fuel* **54** (1975) 249.
82. D. R. JOHNSON and W. A. ROBB, *Amer. Mineral.* **58** (1973) 778.
83. D. R. JOHNSON, *USBM Rept. Inv.* 7862 (1974).
84. J. W. SMITH, Private communication (1977).
85. J. R. DYNI, W. MOUNTJOY, P. L. HAUFF and P. D. BLACKMAN, U. S. Geol. Surv. Prof. Paper No. 750 B (1971).
86. J. W. SAVAGE and D. BAILEY in "Symposium on Chem. Eng. Approaches to Mineral Processing" (Los Angeles, 1968).
87. F. C. LOUGHMAN and G. T. SEE, *Amer. Mineral.* **52** (1967) 1216.
88. C. W. HUGGINS and T. E. GREEN, *ibid.* **58** (1973) 548.
89. E. E. JUKKOLA, A. J. DENILAULER, H. B. JENSEN, W. I. BARNET and W. I. R. MURPHY, *Ind. Eng. Chem.* **45** (1953) 2711.
90. C. W. BECK, Ph.D. Thesis, Harvard University, (1946).
91. T. W. HOWIE and J. R. LAKIN, *Trans. Br. Ceram. Soc.* **46** (1967) 14.
92. G. T. FAUST, *Amer. Mineral.* **35** (1950) 207.
93. R. M. GRUVER, *J. Amer. Ceram. Soc.* **33** (1950) 96.
94. *Idem, ibid.* **33** (1950) 171.
95. J. L. KULP, P. KENT and P. F. KERR, *Amer. Mineral.* **36** (1951) 643.
96. Y. OHNO and S. FUJIYAMA, *Gypsum Lime* **1** (1954) 595.
97. Y. OHNO, *J. Ceram. Assoc. Japan* **62** (1954) 764.
98. T. L. WEBB, DSc. Thesis, University of Pretoria, South Africa (1958).
99. E. G. MALKHASYAN, *Dokl. Akad. Nauk. Armyan SSR* **226** (1958) 297.
100. A. B. RAO, *Arqs. Geol. Univ. Recife* **1** (1959) 37.
101. H. HASHIMOTO and M. ITO, *J. Chem. Soc. Japan, Ind. Chem. Sect.* **65** (1962) 860.
102. W. SMYKATZ-KLOSS, *Beitr. Miner. Petrogr.* **9** (1964) 481.
103. M. S. RAO and S. R. YOGANARASIMHAN, *Amer. Mineral.* **50** (1965) 1489.
104. R. A. W. HAUL and H. HEYSTEK, *ibid.* **37** (1952) 166.
105. D. L. GRAF, *ibid.* **37** (1952) 1.
106. T. L. WEBB and H. HEYSTEK in "Differential Thermal Investigations of Clays," edited by R. C. MacKenzie (Mineralogical Society, London, 1957) p. 329.
107. L. G. BERG, *Dokl. Akad. Nauk. SSSR* **38** (1943) 24.
108. R. A. ROWLAND and D. R. LEWIS, *Amer. Mineral.* **36** (1951) 80.
109. R. L. STONE, *J. Amer. Ceram. Soc.* **37** (1954) 46.
110. J. W. SMITH, D. R. JOHNSON and M. MÜLLER-VONMOOS, *Thermochim. Acta.* **8** (1974) 45.
111. P. A. LANGE and W. ROERKY, *Ber. dt. Keram. Ges* **41** (1964) 497.
112. F. CHANTRET, A. GUILLAMANT and R. POUGET, Comm. Energie At (France) Rappt. No. 2203 (1962).
113. F. PAULIK, J. PAULIK and L. ERDEY, *Acta. Chim. Acad. Sci. Hung.* **26** (1961) 143.
114. C. W. BECK, *Amer. Mineral.* **35** (1950) 985.
115. R. C. MACKENZIE, *Mineral. Mag.* **31** (1957) 681.
116. R. C. MACKENZIE, G. F. WALKER and R. HART, *ibid.* **28** (1969) 704.
117. R. C. MACKENZIE in "The Differential Thermal Investigation of Clays," edited by R. C. MacKenzie (Mineralogical Society, London, 1957) p. 299.
118. A. I. TSVETKOV, E. P. VALYASHIKHINA, and A. D. LASKOVA, *Trudy Inst. Geol. rudn. Mestdrozh.* **42** (1960) 21.
119. W. LODDING in "Thermal Analysis," edited by R. F. Schwenker, Jr., and P. D. Garn (Academic Press, New York, 1969) p. 1239.
120. Y. SCHWOB, *Publs. Tech. Cent. Etud. Rich. Ind. Liants. Hydraul.* **22** (1950).
121. R. A. ROWLAND and E. C. JONAS, *Amer. Mineral.* **34** (1949) 550.
122. J. PAPAILHAU, *Bull. Soc. Franc. Miner. Crist.* **82** (1959) 367.
123. M. L. KEITH and O. F. TUTTLE, *Amer. J. Sci., Bowen Volume,* Part I, (1952) 203.
124. O. BOLGUI and A. DUMITRESCU, *Silic. Ind.* **25** (1960) 517.

125. W. SMYKATZ-KLOSS, "Differential Thermal Analysis" (Springer-Verlag, Berlin, 1974).
126. S. S. TIHEN, H. C. CARPENTER and H. W. SOHNS, *NBS. Special Publ.* **302** (1968) 529.
127. M. PRATS and S. M. O'BRIEN, *J. Pet. Tech.* (1975) 97.
128. R. NOTTENBURG, K. RAJESHWAR, R. ROSENVOLD and J. DUBOW, *Fuel* **57** (1978) 789.
129. T. SLADEK, Ph.D. Thesis, Colorado School of Mines, Golden (1970).
130. C. YOUNG, Private communication (1978).
131. H. LESSER, G. BRUCE and H. STONE, *Quart. Colorado School of Mines* **62** (1967) 111.
132. A. L. BARNES and R. T. ELLINGTON, *ibid.* **63** (1968) 827.
133. M. J. GAVIN and L. H. SHARP, *USBM Rept. Inv.* **2152** (1920).
134. G. W. THOMAS, *Soc. Pet. Eng. J.* (1966).
135. M. Ya. GUBERGRITS, "Thermal Processing of Shale Kukersite," (in Russian) (Tallin, 1966).
136. G. N. SKRYNNIKOVA, E. S. AVDONINA, M. M. GOLYAND and L. Ya. AKHMEDOVA, *Trudy Vsesoyuz Nauch-Issledovatel Inst. Pererabotke Slantsev* 7 (1959) 80.
137. Y. WANG, J. DUBOW, K. RAJESHWAR and R. NOTTENBURG, *Thermochim. Acta* **28** (1979) 23.
138. Y. WANG, K. RAJESHWAR, R. NOTTENBURG and J. DUBOW, *ibid.* **30** (1979) 141.
139. R. J. SHAW, *USBM Rept. Inv.* **4151** (1947).
140. R. F. CANE, *Royal Soc. New South Wales J. and Proc.* **76** (1943) 190.
141. R. L. WISE, R. C. MILLER and H. W. SOHNS, *USBM Rept. Inv.* **7482** (1971).
142. E. W. COOK, *Quart. Colorado School of Mines* **65** (1970) 133.
143. T. A. HENDRICKSON (editor), "Synthetic Fuels Data Handbook" (Cameron Engineers, Inc., Denver, Colorado, 1975).
144. H. W. SOHNS, L. E. MITCHELL, R. J. COX, W. I. BARNET and W. I. R. MURPHY, *Ind. Eng. Chem.* **43** (1951) 33.
145. R. H. MCKEE and E. E. LYDER, *Ind. Eng. Chem.* **13** (1921) 678.
146. R. F. CANE, *Aust. Chem. Inst. Jour. Proc.* **62** (1948).
147. N. I. ZELININ, V. S. FAINBERG and K. B. CHERNYSHEVA, "Chemistry and Technology of Shale Tar" (INSDOC, New Delhi, 1976).
148. P. R. TISOT, *J. Chem. Eng. Data* 7 (1962) 405.
149. G. U. DINNEEN, paper presented at the UN Symposium on the Development and Utilization of Oil Shale Resources, Tallinn (1968).
150. P. R. TISOT, *USBM Rept. Inv.* **8021** (1975).
151. P. R. TISOT and H. W. SOHNS, *USBM Rept. Inv.* **7576** (1971).
152. E. L. BURWELL, S. S. TIHEN and H. W. SOHNS, *USBM Rept. Inv.* **7860** (1974).
153. P. R. TISOT, *J. Chem. Eng. Data* **12** (1967) 405.
154. V. D. ALLRED, *Quart. Colorado School of Mines* **59** (1964) 47.
155. G. U. DINNEEN, ASME Winter Meeting, New York (1972).
156. J. W. SMITH and D. R. JOHNSON, *ACS Preprints, Div. Fuel Chem.* (1976) 25.
157. R. NOTTENBURG, K. RAJESHWAR, R. ROSENVOLD, and J. DUBOW, *Fuel* **58** (1969) 144.
158. A. A. AGROSKIN and I. G. PETRENKO, *Zavodskaya Lab.* **14** (1948) 807.
159. *Idem, Izv. Akad. Nauk. SSSR, Otdel Tekh. Nauk.* (1950) 89.
160. J. H. SCOTT, R. D. CARROLL and D. R. CUNNINGHAM, *J. Geophys. Res.* **72** (1967) 5101.
161. K. RAJESHWAR, R. NOTTENBURG, J. DUBOW and R. ROSENVOLD, *Thermochim. Acta* **27** (1978) 357.
162. I. M. HODGE, M. D. INGRAM, and A. R. WEST, *J. Electroanal. Chem.* **74** (1976) 125.
163. A. J. PIWINSKII and A. DUBA, *Inst. J. Rock. Mech. Min. Sci. and Geomech. Abstr.* **13** (1976) 165.
164. R. NOTTENBURG, K. RAJESHWAR, M. FREEMAN and J. DUBOW, *Thermochim. Acta* **31** (1979) 39.
165. A. JUDZIS Jr, Ph.D. Dissertation, University of Michigan, Ann Arbor (1978).
166. R. NOTTENBURG, M. FREEMAN and K. RAJESHWAR, Unpublished results (1978).
167. G. T. TSAO, *Ind. Eng. Chem.* **53** (1961) 395.
168. S. C. CHENG and R. I. VACHON, *Int. J. Heat and Mass Transfer* **12** (1969) 249.
169. Y. WANG, K. RAJESHWAR and J. DUBOW. *J. Appl. Phys.* (1979) in press.
170. J. C. MAXWELL, "A Treatise on Electricity and Magnetism," 2nd edition, Vol. 1 (Clarendon Press, Oxford, 1881) p. 398.
171. A. D. BRAILSFORD and K. G. MAJOR, *Brit. J. Appl. Phys.* **15** (1964) 313.
172. T. F. YEN in "Oil Shale," edited by T. F. Yen and G. V. Chilingarian (Elsevier Publishing Co., Amsterdam, 1976) Ch. 7.
173. J. J. SCHMIDT-COLLERUS and C. H. PRIEN in "Science and Technology of Oil Shale," edited by T. F. Yen (Ann Arbor Science Publishers, Michigan, 1976) p. 183.

Received 26 January and accepted 8 February 1979.